TECHNISCHE UNIVERSITÄT CHEMNITZ

Ulrike Baur, Christopher Beattie, Peter Benner,
and Serkan Gugercin

Interpolatory Projection Methods for Parameterized Model Reduction

CSC/09-08

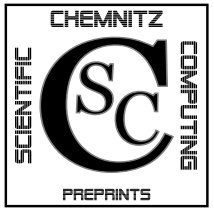

Chemnitz Scientific Computing Preprints

Chemnitz Scientific Computing Preprints – ISSN 1864-0087

Impressum:

Chemnitz Scientific Computing Preprints — ISSN 1864-0087

(1995–2005: Preprintreihe des Chemnitzer SFB393)

Herausgeber:
Professuren für
Numerische und Angewandte Mathematik
an der Fakultät für Mathematik
der Technischen Universität Chemnitz

Postanschrift:
TU Chemnitz, Fakultät für Mathematik
09107 Chemnitz
Sitz:
Reichenhainer Str. 41, 09126 Chemnitz

`http://www.tu-chemnitz.de/mathematik/csc/`

[35] A. Lepschy, G.A. Mian, G. Pinato, and U. Viaro, *Rational L^2 approximation: a non-gradient algorithm*, in Proceedings of the 30th IEEE Conference on Decision and Control, 1991, pp. 2321–2323.

[36] A.T.-M. Leung and R. Khazaka, *Parametric model order reduction technique for design optimization*, in IEEE Internat. Symposium on Circuits and Systems (ISCAS)., May 2005, pp. 1290–1293.

[37] M. Ma, A.T.-M. Leung, and R. Khazaka, *Sparse macromodels for parametric networks*, in IEEE Internat. Symposium on Circuits and Systems (ISCAS)., May 2006, pp. 2545–2548.

[38] Y. Maday and E. M. Rønquist, *A reduced-basis element method.*, C. R., Math., Acad. Sci. Paris, 335 (2002), pp. 195–200.

[39] L. Meier III and D. Luenberger, *Approximation of linear constant systems*, IEEE Trans. Automat. Control, 12 (1967), pp. 585–588.

[40] K. Moosmann and J.G. Korvink, *Automatic parametric MOR for MEMS design*, in Tagungsband GMA-FA 1.30 "Modellbildung, Identifikation und Simulation in der Automatisierungstechnik", Workshop am Bostalsee, 27.–29.9.2006, B. Lohmann and A. Kugi, eds., 2006, pp. 89–99.

[41] J.T. Spanos, M.H. Milman, and D.L. Mingori, *A new algorithm for L^2 optimal model reduction*, Automatica (Journal of IFAC), 28 (1992), pp. 897–909.

[42] M.L. Stein, *Interpolation of Spatial Data: Some Theory for Kriging*, Springer-Verlag, New York, 1999.

[43] P. Van Dooren, K.A. Gallivan, and P.-A. Absil, *$\mathcal{H}_2$-optimal model reduction of MIMO systems*, Appl. Math. Lett., 21 (2008), pp. 1267–1273.

[44] D.S. Weile, E. Michielssen, E.J. Grimme, and K.A. Gallivan, *A method for generating rational interpolant reduced order models of two-parameter linear systems*, Appl. Math. Lett., 12 (1999), pp. 93–102.

[45] D.A. Wilson, *Optimum solution of model-reduction problem*, Proc. Inst. Elec. Eng., 117 (1970), pp. 1161–1165.

[46] W.Y. Yan and J. Lam, *An approximate approach to h^2 optimal model reduction*, IEEE Trans. Automat. Control, 44 (1999), pp. 1341–1358.

[47] A. Yousuff and R.E. Skelton, *Covariance equivalent realizations with applications to model reduction of large-scale systems*, Control and Dynamic Systems, 22 (1985), pp. 273–348.

[48] A. Yousuff, D. Wagie, and R.E. Skelton, *Linear system approximation via covariance equivalent realizations*, J. Math. Anal. Appl., 106 (1985), pp. 91–115.

[49] C. Zenger, *Sparse grids*, in Parallel algorithms for partial differential equations (Kiel, 1990), vol. 31 of Notes Numer. Fluid Mech., Vieweg, Braunschweig, 1991, pp. 241–251.

[50] D. Zigic, L.T. Watson, and C.A. Beattie, *Contragredient transformations applied to the optimal projection equations*, Linear Algebra Appl., 188 (1993), pp. 665–676.

TECHNISCHE UNIVERSITÄT CHEMNITZ

Chemnitz Scientific Computing Preprints

Ulrike Baur, Christopher Beattie, Peter Benner, and Serkan Gugercin

Interpolatory Projection Methods for Parameterized Model Reduction

CSC/09-08

Abstract

We provide a unifying projection-based framework for structure-preserving interpolatory model reduction of parameterized linear dynamical systems, i.e., systems having a structured dependence on parameters that we wish to retain in the reduced-order model. The parameter dependence may be linear or nonlinear and is retained in the reduced-order model. Moreover, we are able to give conditions under which the gradient and Hessian of the system response with respect to the system parameters is matched in the reduced-order model. We provide a systematic approach built on established interpolatory $\mathcal{H}_2$ optimal model reduction methods that will produce parameterized reduced-order models having high fidelity throughout a parameter range of interest. For single input/single output systems with parameters in the input/output maps, we provide reduced-order models that are *optimal* with respect to an $\mathcal{H}_2 \otimes \mathcal{L}_2$ joint error measure. The capabilities of these approaches are illustrated by several numerical examples from technical applications.

This work was supported by DFG grant BE 2174/7-1, *Automatic, Parameter-Preserving Model Reduction for Applications in Microsystems Technology* and NSF Grants DMS-0505971 and DMS- 0645347.

CSC/09-08 **ISSN 1864-0087** **November 2009**

Contents

1 Introduction **1**

2 Problem Setting **2**

3 Interpolatory Model Reduction **3**

4 Interpolatory Model Reduction of Parameterized Systems **5**

5 An $\mathcal{H}_2$-based approach to parameterized model reduction **9**
5.1 Optimal interpolation for special SISO parameterizations 10

6 Numerical Examples **14**
6.1 Convection-diffusion flow in two dimensions 14
6.1.1 Comparison with other model reduction approaches 16
6.2 Thermal conduction in a semiconductor chip 19
6.2.1 Comparison with piecewise balanced truncation 21
6.3 Optimal SISO Parameterized Model Reduction Example 22

7 Conclusions **23**

Christopher Beattie and Serkan Gugercin are with the Department of Mathematics, Virginia Tech., Blacksburg, VA, 24061-0123, USA, [beattie,gugercin]@math.vt.edu.
Ulrike Baur and Peter Benner are with the Fakultät für Mathematik, TU Chemnitz, D-09107 Chemnitz, Germany, [benner,ulrike.baur]@mathematik.tu-chemnitz.de.

[19] L. Feng, E.B. Rudnyi, and J.G. Korvink, *Preserving the film coefficient as a parameter in the compact thermal model for fast electrothermal simulation*, IEEE Trans. Comput.-Aided Des. Integr. Circuits Syst., 24 (2005), pp. 1838–1847.

[20] K. Gallivan, E.J. Grimme, and P. Van Dooren, *Asymptotic waveform evaluation via a Lanczos method*, Appl. Math. Lett., 7 (1994), pp. 75–80.

[21] K. Gallivan, A. Vandendorpe, and P. Van Dooren, *Model reduction of MIMO systems via tangential interpolation*, SIAM J. Matrix Anal. Appl., 26 (2005), pp. 328–349.

[22] M. A. Grepl, Y. Maday, N. C. Nguyen, and A. T. Patera, *Efficient reduced-basis treatment of nonaffine and nonlinear partial differential equations.*, ESAIM, Math. Model. Numer. Anal., 41 (2007), pp. 575–605.

[23] M. Griebel, *Sparse grids and related approximation schemes for higher dimensional problems.* Pardo, Luis M. (ed.) et al., Foundations of computational mathematics, Santander 2005. Selected papers based on the presentations at the international conference of the Foundations of Computational Mathematics (FoCM), Santander, Spain, June 30 – July 9, 2005. Cambridge: Cambridge University Press. London Mathematical Society Lecture Note Series 331, 106–161 (2006)., 2006.

[24] E.J. Grimme, *Krylov projection methods for model reduction*, PhD thesis, Univ. of Illinois at Urbana-Champaign, USA, 1997.

[25] S. Gugercin, A.C. Antoulas, and C.A. Beattie, *$\mathcal{H}_2$ model reduction for large-scale linear dynamical systems*, SIAM J. Matrix Anal. Appl., 30 (2008), pp. 609–638.

[26] P.K. Gunupudi, R. Khazaka, and M.S. Nakhla, *Analysis of transmission line circuits using multidimensional model reduction techniques*, IEEE Trans. Adv. Packaging, 25 (2002), pp. 174–180.

[27] P.K. Gunupudi, R. Khazaka, M.S. Nakhla, T. Smy, and D. Celo, *Passive parameterized time-domain macromodels for high-speed transmission-line networks*, IEEE Trans. Microwave Theory and Techniques, 51 (2003), pp. 2347–2354.

[28] B. Haasdonk, M. Ohlberger, and G. Rozza, *A reduced basis method for evolution schemes with parameter-dependent explicit operators.*, ETNA, Electron. Trans. Numer. Anal., 32 (2008), pp. 145–161.

[29] Y. Halevi, *Frequency weighted model reduction via optimal projection*, IEEE Trans. Automat. Control, 37 (1992), pp. 1537–1542.

[30] D. Hyland and D. Bernstein, *The optimal projection equations for model reduction and the relationships among the methods of Wilson, Skelton, and Moore*, IEEE Trans. Automat. Control, 30 (1985), pp. 1201–1211.

[31] K. Ito and S.S. Ravindran, *A reduced basis method for control problems governed by PDEs.* Desch, W. (ed.) et al., Control and estimation of distributed parameter systems. International conference in Vorau, Austria, July 14–20, 1996. Basel: Birkhäuser. ISNM, Int. Ser. Numer. Math. 126, 153–168 (1998)., 1998.

[32] D.R. Jones, *A taxonomy of global optimization methods based on response surfaces*, J. Global Optim., 21 (2001), pp. 345–383.

[33] D.G. Krige, *A statistical approach to some basic mine valuation problems on the Witwatersrand*, J. Chemical, Metallurgical and Mining Society of South Africa, 52 (1951), pp. 119–139.

[34] C.J.M. Lasance, *Two benchmarks to facilitate the study of compact thermal modelingphenomena*, IEEE Trans. Components and Packaging Technologies, 24 (2001), pp. 559–565.

15 (1998), pp. 16–23.

[2] M. Barrault, Y. Maday, N. C. Nguyen, and A. T. Patera, *An 'empirical interpolation' method: Application to efficient reduced-basis discretization of partial differential equations.*, C. R., Math., Acad. Sci. Paris, 339 (2004), pp. 667–672.

[3] U. Baur and P. Benner, *Model Reduction for Parametric Systems Using Balanced Truncation and Interpolation*, at-Automatisierungstechnik, 57 (2009), pp. 411–420. In German.

[4] C.A. Beattie and S. Gugercin, *Interpolatory Projection Methods for Structure-preserving Model Reduction*, Sys. Control Lett., 58 (2008), pp. 225–232.

[5] P. Benner and L. Feng, *A robust algorithm for parametric model order reduction based on implicit moment matching*. Submitted.

[6] B. Bond and L. Daniel, *Parameterized model order reduction of nonlinear dynamical systems*, in IEEE/ACM Internat.Conf. on Computer-Aided Design, 2005. ICCAD-2005, 2005, pp. 487–494.

[7] A. Bryson, *Second-order algorithm for optimal model order reduction*, J. Guidance, Control, Dynamics, 13 (1990), pp. 887–892.

[8] T. Bui-Thanh, K. Willcox, and O. Ghattas, *Model reduction for large-scale systems with high-dimensional parametric input space*, SIAM J. Sci. Comput., 30 (2008), pp. 3270–3288.

[9] H-J. Bungartz and M. Griebel, *Sparse grids.*, Acta Numerica, 13 (2004), pp. 147–269.

[10] A. Bunse-Gerstner, D. Kubalinska, G. Vossen, and D. Wilczek, *$\mathcal{H}_2$-optimal model reduction for large scale discrete dynamical MIMO systems*, to appear in J. Comput. Appl. Math., (2007). In Press, available online: http://dx.doi.org/10.1016/j.cam.2008.12.029.

[11] D.G. Cacuci, *Sensitivity and uncertainty analysis. Vol. I: Theory*, Chapman & Hall/CRC, Boca Raton, FL, 2003.

[12] L. Daniel, O.C. Siong, L.S. Chay, K.H. Lee, and J. White, *A multiparameter moment-matching model-reduction approach for generating geometrically parameterized interconnect performance models*, IEEE Trans. Comput.-Aided Des. Integr. Circuits Syst., 23 (2004), pp. 678–693.

[13] C. De Villemagne and R.E. Skelton, *Model reductions using a projection formulation*, Internat. J. Control, 46 (1987), pp. 2141–2169.

[14] R. Eid, B. Salimbahrami, B. Lohmann, E.B. Rudnyi, and J.G. Korvink, *Parametric order reduction of proportionally damped second-order systems*, in Sensors and Materials, Tokyo, vol. 19, 2007, pp. 149–164.

[15] O. Farle, V. Hill, P. Ingelström, and R. Dyczij-Edlinger, *Multi-parameter polynomial order reduction of linear finite element models*, Math. Comput. Model. Dyn. Syst., 14 (2008), pp. 421–434.

[16] P. Feldmann and R.W. Freund, *Efficient linear circuit analysis by Padé approximation via the Lanczos process*, IEEE Trans. Comput.-Aided Des. Integr. Circuits Syst., 14 (1995), pp. 639–649.

[17] L. Feng, *Parameter independent model order reduction*, Math. Comput. Simulation, 68 (2005), pp. 221–234.

[18] L. Feng and P. Benner, *A robust algorithm for parametric model order reduction based on implicit moment matching*, Proc. Appl. Math. Mech., 7 (2008), pp. 1021501–1021502.

1 Introduction

The importance of numerical simulation has steadily increased across virtually all scientific and engineering disciplines. In many application areas, experiments have been largely replaced by numerical simulation in order to save costs in design and development. High accuracy simulation requires high fidelity mathematical models which in turn induce dynamical systems of very large dimension. The ensuing demands on computational resources can be overwhelming and efficient model utilization becomes a necessity. It often is both possible and prudent to produce a lower dimension model that approximates the response of the original one to high accuracy. There are many model reduction strategies in use that are remarkably effective in the creation of compact, efficient, and high-fidelity dynamical system models. Such a reduced model can then be used reliably as an efficient surrogate to the original system, replacing it as a component in larger simulations, for example, or in allied contexts that involve design optimization or the development of low-order, fast controllers suitable for real time applications.

Typically, a reduced-order model will represent a specific instance of the physical system under study and as a consequence will have high fidelity only for small variations around that base system instance. Significant modifications to the physical model such as geometric variations, changes in material properties, or alterations in boundary conditions generally necessitate generation of new reduced models. This can be particularly onerous in design optimization where parameters are changed in each optimization cycle. Since the generation of a high fidelity reduced model may be comparable in expense to a (brief) simulation of an instance of the original full-order model, the benefits of model reduction will be fully realized only if the parametric dependence found in the original dynamical system can be preserved in some fashion within the reduced model. This is the goal of *parameterized model reduction (PMOR)*: generate a dynamical system of reduced order which retains a functional dependence on important design parameters and recovers the response of the original full-order dynamical system with high fidelity throughout the range of interest of the design parameters.

Many design optimization approaches utilize surrogate models that are constructed using response surface modeling or Kriging [33, 32, 42]. These techniques are very flexible, broadly applicable, and can be efficient for uncertain, unstructured, or empirically-based models, but they generally cannot exploit fully the character of time-dependent processes generated by an underlying dynamical system. PMOR is an approach that attempts to take direct account of structure in the underlying dynamical system that is creating the response data. Thus it can be expected to produce more efficient and accurate models than general purpose approaches that provide *ad hoc* fits or regressions to observed input/output responses.

PMOR is at an early stage of the development. Currently there are developments based on multivariate Padé approximation [5, 6, 12, 14, 15, 17, 18, 19, 27, 26, 36, 37, 40, 44]. These methods differ in the way moments are computed (implicitly vs explicity) and in the number of (mixed) moments that are matched. Approaches based on explicitly computed moments suffer from the same numerical instabilities as analogous methods for model reduction of nonparameterized systems. However implicit approaches appear to provide a robust resolution of these difficulties at least for low dimensional parameter spaces. Moment-matching properties can be proved (see [5]) analogously as for standard moment-matching methods like Padé-via-Lanczos [16, 20]. Other approaches include interpolation of the transfer function, see [3], and reduced basis methods (see, e.g., [2, 22, 28, 31, 38]). Reduced-basis methods are successful in finding an information rich set of global ansatz functions for spatial discretization of parameterized partial differential equations (PDEs). In the setting we consider here, we do not necessarily assume that a PDE is provided, but we start from a parameterized state-space model. This is the case, e.g., when computer aided engineering (CAE) tools for automatic model generation are used. In this situation, the spatial discretization of the PDE is performed inside the CAE tool and reduced basis methods are not directly applicable. Therefore, we will not discuss them here any further.

We lay out our basic problem setting, define notation, and describe precisely in what sense our model reduction methods are structure-preserving in Section 2. In Section 3, we review the particular aspects of interpolatory model reduction in standard (nonparameterized) settings that

are useful for us, focusing especially on the selection of interpolation points that lead to optimal reduced-order models. In Section 4, we derive an interpolation-based approach to PMOR that is closely associated with rational Krylov methods developed by Grimme [24] and earlier work by Villemagne and Skelton [13]. As in these earlier works, interpolation properties are governed by the range and cokernel of a (skew) projection associated with the model reduction process. Remarkably, similar conditions govern the matching of gradient and Hessian information of the system response with respect to the system parameters. Efficient numerical methods built on previously known $\mathcal{H}_2$ optimal model reduction methods are introduced in Section 5 and we describe in Section 5.1 how to find *optimal* parameterized reduced-order models for a special case of a parameterized single input/single output system. The efficiency of the derived numerical algorithms for PMOR is illustrated using several real-world examples from microsystems technology in Section 6.

2 Problem Setting

Consider a multi-input/multi-output (MIMO) linear dynamical system parameterized with ν parameters $\mathbf{p} = [p_1, ..., p_\nu]^T \in \mathbb{R}^\nu$, presented in state space form as:

$$\begin{aligned} \mathbf{E}(\mathbf{p})\,\dot{\mathbf{x}}(t) &= \mathbf{A}(\mathbf{p})\,\mathbf{x}(t) + \mathbf{B}(\mathbf{p})\,\mathbf{u}(t), \\ \mathbf{y}(t) &= \mathbf{C}(\mathbf{p})\,\mathbf{x}(t), \end{aligned} \qquad \text{with } \mathbf{x}(0) = 0, \tag{1}$$

where $\mathbf{E}(\mathbf{p}),\ \mathbf{A}(\mathbf{p}) \in \mathbb{R}^{n\times n}$, $\mathbf{B}(\mathbf{p}) \in \mathbb{R}^{n\times m}$, and $\mathbf{C}(\mathbf{p}) \in \mathbb{R}^{\ell\times n}$. Our framework allows parameter dependency in all system matrices. Without loss of generality, assume the parametric dependence in the system matrices of (1) has the following form:

$$\begin{aligned} \mathbf{E}(\mathbf{p}) &= \mathbf{E}_0 + e_1(\mathbf{p})\mathbf{E}_1 + \ldots + e_M(\mathbf{p})\mathbf{E}_M, \\ \mathbf{A}(\mathbf{p}) &= \mathbf{A}_0 + f_1(\mathbf{p})\mathbf{A}_1 + \ldots + f_M(\mathbf{p})\mathbf{A}_M, \\ \mathbf{B}(\mathbf{p}) &= \mathbf{B}_0 + g_1(\mathbf{p})\mathbf{B}_1 + \ldots + g_M(\mathbf{p})\mathbf{B}_M, \\ \mathbf{C}(\mathbf{p}) &= \mathbf{C}_0 + h_1(\mathbf{p})\mathbf{C}_1 + \ldots + h_M(\mathbf{p})\mathbf{C}_M. \end{aligned} \tag{2}$$

We assume throughout that (1) is stable for all parameter choices $\mathbf{p}$ considered. The parameter dependence encoded in the functions e_j, f_j, g_j, h_j may be linear or nonlinear, but is assumed smooth enough to allow for approximation by interpolation.

The representation (2) is not unique; there may be many ways in which one may express system matrices, $\mathbf{E}(\mathbf{p})$, $\mathbf{A}(\mathbf{p})$, $\mathbf{B}(\mathbf{p})$, and $\mathbf{C}(\mathbf{p})$, in such a form and the number of terms, M, as well as the particular parameter functions e_j, f_j, g_j, h_j may vary with the representation that one chooses. A desirable choice should produce as few terms as possible (M as small as possible) for reasons we describe below; the methods we propose will be most advantageous when $M \ll n$. Note also that the actual number of terms appearing may vary among the matrices $\mathbf{E}(\mathbf{p})$, $\mathbf{A}(\mathbf{p})$, $\mathbf{B}(\mathbf{p})$, and $\mathbf{C}(\mathbf{p})$.

A general projection framework for structure-preserving PMOR can be described as follows: suppose that (constant) matrices $\mathbf{V}_r,\ \mathbf{W}_r \in \mathbb{C}^{n\times r}$ with $r \ll n$ and $\operatorname{rank}(\mathbf{V}_r) = \operatorname{rank}(\mathbf{W}_r) = r$ are specified and define an associated reduced system:

$$\begin{aligned} \mathbf{E}_r(\mathbf{p})\ \dot{\mathbf{x}}_r(t) &= \mathbf{A}_r(\mathbf{p})\,\mathbf{x}_r(t) + \mathbf{B}_r(\mathbf{p})\,\mathbf{u}(t), \\ \mathbf{y}_r(t) &= \mathbf{C}_r(\mathbf{p})\,\mathbf{x}_r(t) \qquad \text{with } \mathbf{x}_r(0) = 0, \\ \text{where}\quad \mathbf{E}_r(\mathbf{p}) &= \mathbf{W}_r^T\mathbf{E}(\mathbf{p})\mathbf{V}_r, \quad \mathbf{A}_r(\mathbf{p}) = \mathbf{W}_r^T\mathbf{A}(\mathbf{p})\mathbf{V}_r, \\ \mathbf{B}_r(\mathbf{p}) &= \mathbf{W}_r^T\mathbf{B}(\mathbf{p}), \quad \text{and} \quad \mathbf{C}_r(\mathbf{p}) = \mathbf{C}(\mathbf{p})\mathbf{V}_r. \end{aligned} \tag{3}$$

The parametric dependence of the original system (1) is retained in the reduced system (3) in the

region of interest. The 10^{th} order optimal parameterized reduced-order model yields an extremely satisfactory relative $\mathcal{H}_2 \otimes \mathcal{L}_2(\mathcal{D})$ error of 7.54×10^{-4}.

To show the superiority of this optimal selection for the introduced $\mathcal{H}_2 \otimes \mathcal{L}_2(\mathcal{D})$ measure, we compare the results with those obtained by the $\mathcal{H}_2$-based method in Algorithm 5.1, i.e. we choose $[0,0]^T$, $[0,0.5]^T$, $[0.5,0]^T$ and $[1,1]^T$ as parameter vectors, use $\mathcal{H}_2$ optimal reduced-order models at each parameter set and then combine the resulting subspaces together. The resulting reduced-order model of order $r = 10$ leads to a relative $\mathcal{H}_2 \otimes \mathcal{L}_2(\mathcal{D})$ error of 2.09×10^{-2}. Even though this is a satisfactory relative error, the result using the optimal points is two order of magnitudes better, illustrating the superiority of the $\mathcal{H}_2 \otimes \mathcal{L}_2(\mathcal{D})$ optimal point selection.

Even though the $\mathcal{H}_2 \otimes \mathcal{L}_2(\mathcal{D})$ optimal approach does not minimize the $\mathcal{H}_2$ error at every point in the parameter range, we compare the quality of the derived results by computing the relative $\mathcal{H}_2$ error (34) over the full parameter range. The results are shown in Figure 12. The $\mathcal{H}_2 \otimes \mathcal{L}_2(\mathcal{D})$ optimal approach yields much smaller $\mathcal{H}_2$-errors for most of the grid points with a maximum error of 2.04×10^{-2}. On the other hand, the maximum $\mathcal{H}_2$-error due to Algorithm 5.1 is 2.09×10^{-2}.

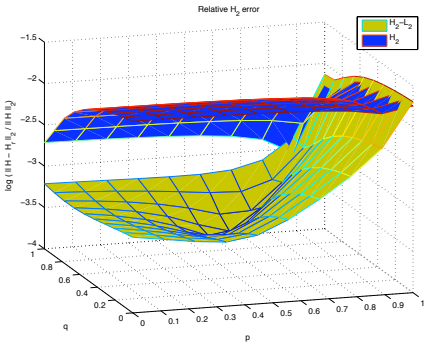

Figure 12: Example C: relative $\mathcal{H}_2$ error as p_1 and p_2 vary.

7 Conclusions

We have introduced a unifying projection-based framework for structure-preserving interpolatory model reduction of parameterized linear dynamical systems. Analogous to the nonparameterized case, we provide conditions under which the transfer functions of original and reduced-order model coincide at interpolation points for the parameter vectors. Furthermore, we are able to give conditions under which the gradient and Hessian of the system response with respect to the system parameters is matched in the reduced-order model. We provide a systematic approach built on established interpolatory $\mathcal{H}_2$-optimal model reduction methods that will produce parameterized reduced-order models having high fidelity throughout a parameter range of interest. For single input/single output systems with parameters in the input/output maps, we provide reduced order models that are optimal with respect to an $\mathcal{H}_2 \otimes \mathcal{L}_2$ joint error measure. The capabilities of these approaches are illustrated by several numerical examples from technical applications.

References

[1] N. Alexandrov, J.E. Dennis, Jr., R.M. Lewis, and V. Torczon, *A trust region framework for managing the use of approximation models in optimization*, Structural Optimization,

Cases:		A	B	C	D	E	F	G
dim. at $\mathbf{p}^{(i)}$	r_1	4	5	6	7	7	6	8
	r_2	4	5	4	4	5	6	7
Total dim: r $\mathbf{H}_r/\mathbf{H}_{\text{bal}}$		6/6-8	9/9	9/10	10/11	10/12	11/12	14/14
Max. rel. $\mathcal{H}_\infty$-err.	$\mathbf{H}_r$	1.87 E-1	6.69 E-2	9.75 E-2	8.29 E-2	6.88 E-2	3.50 E-2	2.16 E-2
	$\mathbf{H}_{\text{bal}}$	∞	2.65 E-2	5.23 E-2	5.09 E-2	4.73 E-2	2.47 E-2	4.56 E-2

Table 3: $\mathbf{H}_r$: Piecewise $\mathcal{H}_2$ optimal reduced model; $\mathbf{H}_{\text{bal}}$: Piecewise balanced truncation reduced model

using balanced truncation for the fixed parameter vectors $\mathbf{p}^{(1)}$ and $\mathbf{p}^{(2)}$. To give an overall picture, we use many different combinations of r_1 and r_2 values and then compute maximum relative $\mathcal{H}_\infty$ errors encountered while varying p_1 and p_2 over the full parameter range of $[1,\ 10^4]$. The results are tabulated in Table 3 where ∞ corresponds to encountering some unstable reduced-order models while p_1 and p_2 vary. One obvious conclusion is that the proposed $\mathcal{H}_2$-based method consistently yields results that are as accurate as those obtained by the balancing-based approach. Note that the error values are computed using the $\mathcal{H}_\infty$ norm. Hence, the proposed $\mathcal{H}_2$-based approach yields accurate reduced-model not only in the $\mathcal{H}_2$ norm but also in the $\mathcal{H}_\infty$ norm. This is not surprising since the optimal $\mathcal{H}_2$ method described in Algorithm 3.1 for nonparameterized systems is known to yield both good $\mathcal{H}_\infty$ performance and $\mathcal{H}_2$ performance, see [25].

6.3 Optimal SISO Parameterized Model Reduction Example

In this example, we illustrate the concepts introduced in Section 5.1. The full-order model of form (23) represents the heat distribution on a plate and is described by the heat equation. A model of order 197 is obtained by spatial discretization. The vectors $\mathbf{b}_0$ and $\mathbf{b}_1$ correspond to the location of the heat source. As the parameter q varies from 0 to 1, the input shifts from one heat source to the other. Similarly, the vectors $\mathbf{c}_0$ and $\mathbf{c}_1$ represent point measurements and as the parameter p varies from 0 to 1, the location of the measurement changes.

We minimize the $\mathcal{H}_2 \otimes \mathcal{L}_2(\mathcal{D})$ error between the full-order and the reduced-order transfer functions as shown in Theorem 7 by applying Algorithm 5.2. The corresponding MIMO non-parameterized systems in line 2 of the algorithm are reduced to order $r = 10$ by $\mathcal{H}_2$ optimal model reduction in Algorithm 3.1. The resulting optimal frequency shifts, $\{-\tilde{\lambda}_i\}_{i=1}^r$, and *optimal parameter interpolation vectors*, $\{\widetilde{\mathbf{p}}^{(i)}\}_{i=1}^r$ are given below:

$-\tilde{\lambda}_i$	$\widetilde{\mathbf{p}}^{(i)}$	
	p_i	q_i
0.0152	0.559	0.344
0.142	0.246	0.351
0.416	−0.516	0.359
0.862	0.454	0.337
0.102	0.620	0.310
0.184	0.549	0.385
0.419	0.512	0.366
28.9	0.349	0.319
$7.24 - \imath\, 1.10$	$0.435 + \imath\, 0.0404$	$0.406 - \imath\, 0.0778$
$7.24 + \imath\, 1.10$	$0.435 - \imath\, 0.0404$	$0.406 + \imath\, 0.0778$

An interesting observation is that even though both parameters p and q are contained in the interval $[0,\ 1]$, *some of the optimal parameter values lie outside this region, indeed some of the optimal points are even complex*. This example is a perfect illustration of the fact that the best parameter selection does not necessarily lies in the parameter range; i.e., one can obtain a better performance by including complex parameter points or at least parameter values outside the

sense that

$$\begin{aligned}
\mathbf{E}_r(\mathbf{p}) &= \mathbf{W}_r^T\mathbf{E}_0\mathbf{V}_r + e_1(\mathbf{p})\mathbf{W}_r^T\mathbf{E}_1\mathbf{V}_r + \cdots + e_M(\mathbf{p})\mathbf{W}_r^T\mathbf{E}_M\mathbf{V}_r,\\
\mathbf{A}_r(\mathbf{p}) &= \mathbf{W}_r^T\mathbf{A}_0\mathbf{V}_r + f_1(\mathbf{p})\mathbf{W}_r^T\mathbf{A}_1\mathbf{V}_r + \cdots + f_M(\mathbf{p})\mathbf{W}_r^T\mathbf{A}_M\mathbf{V}_r,\\
\mathbf{B}_r(\mathbf{p}) &= \mathbf{W}_r^T\mathbf{B}_0 + g_1(\mathbf{p})\mathbf{W}_r^T\mathbf{B}_1 + \cdots + g_M(\mathbf{p})\mathbf{W}_r^T\mathbf{B}_M,\\
\mathbf{C}_r(\mathbf{p}) &= \mathbf{C}_0\mathbf{V}_r + h_1(\mathbf{p})\mathbf{C}_1\mathbf{V}_r + \cdots + h_M(\mathbf{p})\mathbf{C}_M\mathbf{V}_r,
\end{aligned} \tag{4}$$

which is evidently structurally similar to (2). Once the matrices $\mathbf{V}_r$ and $\mathbf{W}_r$ are specified, all the constituent matrices, $\mathbf{W}_r^T\mathbf{E}_k\mathbf{V}_r$, $\mathbf{W}_r^T\mathbf{A}_k\mathbf{V}_r$, $\mathbf{W}_r^T\mathbf{B}_k$, and $\mathbf{C}_k\mathbf{V}_r$ for $k = 0, \ldots, M$ contributing to $\mathbf{E}_r(\mathbf{p})$, $\mathbf{A}_r(\mathbf{p})$, $\mathbf{B}_r(\mathbf{p})$, and $\mathbf{C}_r(\mathbf{p})$ can be *precomputed*. Although the order, r, of the dynamical system (3) is an obvious point of focus in judging the cost of using the reduced system, the size of M, as a measure of the complexity of the representation (2), may also become a factor since for every new choice of parameter values, the cost of generating $\mathbf{E}_r(\mathbf{p})$, $\mathbf{A}_r(\mathbf{p})$, $\mathbf{B}_r(\mathbf{p})$, and $\mathbf{C}_r(\mathbf{p})$ obviously grows proportionally to M.

Whenever the input $\mathbf{u}(t)$ is exponentially bounded - that is, when there is a fixed $\gamma \in \mathbb{R}$ such that $\|\mathbf{u}(t)\| \sim \mathcal{O}(e^{\gamma t})$, then $\mathbf{x}(t)$ and $\mathbf{y}(t)$ from (1) and $\mathbf{x}_r(t)$ and $\mathbf{y}_r(t)$ from (3) will also be exponentially bounded and the Laplace transform can be applied to (1) and (3) to obtain

$$\widehat{\mathbf{y}}(s,\mathbf{p}) = \mathbf{C}(\mathbf{p})\left(s\,\mathbf{E}(\mathbf{p}) - \mathbf{A}(\mathbf{p})\right)^{-1}\mathbf{B}(\mathbf{p})\,\widehat{\mathbf{u}}(s), \tag{5}$$

$$\widehat{\mathbf{y}}_r(s,\mathbf{p}) = \mathbf{C}_r(\mathbf{p})\left(s\,\mathbf{E}_r(\mathbf{p}) - \mathbf{A}_r(\mathbf{p})\right)^{-1}\mathbf{B}_r(\mathbf{p})\,\widehat{\mathbf{u}}(s), \tag{6}$$

where we have denoted Laplace transformed quantities with "$\widehat{\ }$". We define parameterized transfer functions accordingly:

$$\text{and} \qquad \mathbf{H}(s,\mathbf{p}) = \mathbf{C}(\mathbf{p})\left(s\,\mathbf{E}(\mathbf{p}) - \mathbf{A}(\mathbf{p})\right)^{-1}\mathbf{B}(\mathbf{p}) \tag{7}$$

$$\mathbf{H}_r(s,\mathbf{p}) = \mathbf{C}_r(\mathbf{p})\left(s\,\mathbf{E}_r(\mathbf{p}) - \mathbf{A}_r(\mathbf{p})\right)^{-1}\mathbf{B}_r(\mathbf{p}). \tag{8}$$

The quality of the approximation $\widehat{\mathbf{y}}_r(s,\mathbf{p}) \approx \widehat{\mathbf{y}}(s,\mathbf{p})$ is tied directly to the quality of the approximation $\mathbf{H}_r(s,\mathbf{p}) \approx \mathbf{H}(s,\mathbf{p})$. The quality of this approximation in general, and interpolation properties, in particular, depend entirely on how the matrices $\mathbf{V}_r$ and $\mathbf{W}_r$ are selected.

There is substantial flexibility in choosing $\mathbf{V}_r$ and $\mathbf{W}_r$. We do require that both $\mathbf{V}_r$ and $\mathbf{W}_r$ have full rank but it is not necessary to require that either $\mathbf{W}_r^T\mathbf{V}_r$ or $\mathbf{W}_r^T\mathbf{E}(\mathbf{p})\mathbf{V}_r$ be nonsingular. Note that if $\mathbf{E}(\mathbf{p})$ is nonsingular, then $\mathbf{H}(s,\mathbf{p})$ is a strictly proper transfer function and one may wish $\mathbf{H}_r(s,\mathbf{p})$ to be strictly proper as well — leading to the requirement that $\mathbf{E}_r(\mathbf{p}) = \mathbf{W}_r^T\mathbf{E}(\mathbf{p})\mathbf{V}_r$ be nonsingular as well. This can be thought of as an interpolation condition since under these circumstances $\mathbf{H}_r$ will interpolate $\mathbf{H}$ at infinity: $\lim_{s\to\infty}\mathbf{H}(s) = \lim_{s\to\infty}\mathbf{H}_r(s) = 0$ (facilitating, in effect, a good match between true and reduced-order system response at high frequencies). Although we allow $\mathbf{V}_r$ and $\mathbf{W}_r$ to be complex in order to simplify the discussion, in most circumstances $\mathbf{V}_r$ and $\mathbf{W}_r$ can be chosen to be real so (3) represents a real dynamical system.

3 Interpolatory Model Reduction

Consider a full-order (nonparameterized) dynamical system described by

$$\begin{aligned}
\mathbf{E}\,\dot{\mathbf{x}}(t) &= \mathbf{A}\,\mathbf{x}(t) + \mathbf{B}\,\mathbf{u}(t),\\
\mathbf{y}(t) &= \mathbf{C}\,\mathbf{x}(t),
\end{aligned} \qquad \text{with } \mathbf{x}(0) = 0, \tag{9}$$

where $\mathbf{A}, \mathbf{E} \in \mathbb{R}^{n\times n}$, $\mathbf{B} \in \mathbb{R}^{n\times m}$, and $\mathbf{C} \in \mathbb{R}^{\ell\times n}$ and we have the associated transfer function $\mathbf{H}(s) = \mathbf{C}(s\mathbf{E} - \mathbf{A})^{-1}\mathbf{B}$. We seek a reduced system with state-space form

$$\begin{aligned}
\mathbf{E}_r\,\dot{\mathbf{x}}_r(t) &= \mathbf{A}_r\,\mathbf{x}_r(t) + \mathbf{B}_r\,\mathbf{u}(t),\\
\mathbf{y}_r(t) &= \mathbf{C}_r\,\mathbf{x}_r(t),
\end{aligned} \qquad \text{with } \mathbf{x}_r(0) = 0, \tag{10}$$

and associated transfer function, $\mathbf{H}_r(s) = \mathbf{C}_r(s\mathbf{E}_r - \mathbf{A}_r)^{-1}\mathbf{B}_r$, where $\mathbf{A}_r, \mathbf{E}_r \in \mathbb{C}^{r\times r}$, $\mathbf{B}_r \in \mathbb{C}^{r\times m}$, and $\mathbf{C}_r \in \mathbb{C}^{\ell\times r}$, and $r \ll n$, are such that $\mathbf{y}_r(t)$ approximates $\mathbf{y}(t)$ well. We adopt the projection framework described above, specifying matrices $\mathbf{V}_r \in \mathbb{C}^{n\times r}$ and $\mathbf{W}_r \in \mathbb{C}^{n\times r}$, such that $\text{rank}(\mathbf{V}_r) = \text{rank}(\mathbf{W}_r) = r$, which determine reduced system matrices $\mathbf{E}_r = \mathbf{W}_r^T\mathbf{E}\mathbf{V}_r$, $\mathbf{A}_r = \mathbf{W}_r^T\mathbf{A}\mathbf{V}_r$, $\mathbf{B}_r = \mathbf{W}_r^T\mathbf{B}$, and $\mathbf{C}_r = \mathbf{C}\mathbf{V}_r$.

Interpolatory model reduction is an approach that was introduced by Skelton *et. al.* in [13, 47, 48] and later placed into a numerically efficient framework by Grimme [24]. Gallivan *et al.* [21] developed a more versatile version for MIMO systems, a variant of which we describe and then adapt to parameterized systems: Starting with a full-order system as in (9) and selected interpolation points, σ_k, in the complex plane paired with corresponding left and right directions $\mathbf{c}_k \in \mathbb{C}^\ell$ and $\mathbf{b}_k \in \mathbb{C}^m$, we produce matrices $\mathbf{V}_r \in \mathbb{C}^{n\times r}$ and $\mathbf{W}_r \in \mathbb{C}^{n\times r}$ that define a reduced-order system (10) in such a way that the reduced transfer function, $\mathbf{H}_r(s)$, is a *Hermite interpolant* of the full-order transfer function, $\mathbf{H}(s)$, at each σ_k along both left and right directions:

$$\begin{aligned} \mathbf{c}_i^T\mathbf{H}(\sigma_i) = \mathbf{c}_i^T\mathbf{H}_r(\sigma_i), \quad \mathbf{H}(\sigma_i)\mathbf{b}_i = \mathbf{H}_r(\sigma_i)\mathbf{b}_i, \quad \text{and} \\ \mathbf{c}_i^T\,\mathbf{H}_r'(\sigma_i)\,\mathbf{b}_i = \mathbf{c}_i^T\,\mathbf{H}'(\sigma_i)\,\mathbf{b}_i \quad \text{for } i = 1,\ldots,r. \end{aligned} \tag{11}$$

Since the matrix-valued function, $\mathbf{H}_r(s)$, consists of rational functions in s, (11) describes a *rational interpolation* problem. The following theorem gives elementary subspace criteria forcing interpolation.

Theorem 1. *Let $\sigma \in \mathbb{C}$ be such that both $\sigma\,\mathbf{E} - \mathbf{A}$ and $\sigma\,\mathbf{E}_r - \mathbf{A}_r$ are invertible. If $\mathbf{b} \in \mathbb{C}^m$ and $\mathbf{c} \in \mathbb{C}^\ell$ are fixed nontrivial vectors then*

(a) if $(\sigma\,\mathbf{E} - \mathbf{A})^{-1}\,\mathbf{B}\mathbf{b} \in \text{Ran}(\mathbf{V}_r)$, then $\mathbf{H}(\sigma)\mathbf{b} = \mathbf{H}_r(\sigma)\mathbf{b}$;

(b) if $\left(\mathbf{c}^T\mathbf{C}\,(\sigma\,\mathbf{E} - \mathbf{A})^{-1}\right)^T \in \text{Ran}(\mathbf{W}_r)$, then $\mathbf{c}^T\mathbf{H}(\sigma) = \mathbf{c}^T\mathbf{H}_r(\sigma)$; and

(c) if both $(\sigma\,\mathbf{E} - \mathbf{A})^{-1}\,\mathbf{B}\mathbf{b} \in \text{Ran}(\mathbf{V}_r)$ and $\left(\mathbf{c}^T\mathbf{C}\,(\sigma\,\mathbf{E} - \mathbf{A})^{-1}\right)^T \in \text{Ran}(\mathbf{W}_r)$, then $\mathbf{c}^T\mathbf{H}'(\sigma)\mathbf{b} = \mathbf{c}^T\mathbf{H}_r'(\sigma)\mathbf{b}$.

Theorem 1 makes the solution of (11) straightforward. Given a set of distinct shifts $\{\sigma_k\}_{k=1}^r$, left-tangent directions $\{\mathbf{c}_k\}_{k=1}^r \subset \mathbb{C}^\ell$, and right-tangent directions $\{\mathbf{b}_k\}_{k=1}^r \subset \mathbb{C}^m$, construct full-rank matrices $\mathbf{V}_r$ and $\mathbf{W}_r$ such that

$$\text{Ran}(\mathbf{V}_r) \supseteq \text{span}\{\left[(\sigma_1\mathbf{E} - \mathbf{A})^{-1}\mathbf{B}\mathbf{b}_1,\ \cdots,\ (\sigma_r\mathbf{E} - \mathbf{A})^{-1}\mathbf{B}\mathbf{b}_r\right]\} \tag{12}$$

and

$$\text{Ran}(\mathbf{W}_r) \supseteq \text{span}\{\left[(\mathbf{c}_1^T\mathbf{C}(\sigma_1\mathbf{E} - \mathbf{A})^{-1})^T,\ \cdots,\ (\mathbf{c}_r^T\mathbf{C}(\sigma_r\mathbf{E} - \mathbf{A})^{-1})^T\right]\}. \tag{13}$$

If $\sigma_i\mathbf{E}_r - \mathbf{A}_r$ is nonsingular for each $i = 1,\ldots,r$, then the reduced system $\mathbf{H}_r(s) = \mathbf{C}_r(s\mathbf{E}_r - \mathbf{A}_r)^{-1}\mathbf{B}_r$ defined by $\mathbf{A}_r = \mathbf{W}_r^T\mathbf{A}\mathbf{V}_r$, $\mathbf{E}_r = \mathbf{W}_r^T\mathbf{E}\mathbf{V}_r$, $\mathbf{B}_r = \mathbf{W}_r^T\mathbf{B}$, and $\mathbf{C}_r = \mathbf{C}\mathbf{V}_r$ solves the tangential interpolation problem (11). In [4], Beattie and Gugercin showed how to solve the tangential interpolation problem posed in (11) for a substantially larger class of transfer functions – those having a coprime factorization of the form $\mathbf{H}(s) = \mathbf{C}(s)\mathbf{K}(s)^{-1}\mathbf{B}(s)$ with $\mathbf{B}(s)$, $\mathbf{C}(s)$, and $\mathbf{K}(s)$ given as meromorphic matrix-valued functions. This generalization lays the foundation of our present developments for parametrized model reduction described here.

Interpolatory model reduction methods are computationally advantageous since the principal task that is required is solution of (multiple) linear systems having the form $(\sigma\mathbf{E} - \mathbf{A})\mathbf{v} = \mathbf{B}\mathbf{b}$ or $(\sigma\mathbf{E}^T - \mathbf{A}^T)\mathbf{w} = \mathbf{C}^T\mathbf{c}$. Often one is able to take advantage of sparsity or other special structure in the linear systems.

The fidelity of the final reduced-order model must always be of central concern and clearly the selection of interpolation points and tangent directions becomes the main factor in determining success or failure. Until recently, selection of interpolation points was largely *ad hoc*. Recently however, Gugercin *et al.* [25] showed an optimal shift selection strategy that produces reduced-order

where $\mathbf{E} \in \mathbb{R}^{4257\times4257}$ and $\mathbf{A} \in \mathbb{R}^{4257\times4257}$ are system matrices, $\mathbf{A}_i \in \mathbb{R}^{4257\times4257}$, $i = 1,\ldots,3$, are diagonal matrices arising from the discretization of the convection boundary condition on the ith interface, and $\mathbf{B} \in \mathbb{R}^{4257}$ and $\mathbf{C} \in \mathbb{R}^{7\times4257}$; i.e. the system has a single input and seven outputs. The range for each parameter is the interval $[1,\ 10^4]$. Four important parameter vectors in $[1,\ 10^4]^3$ are given in Table 2 below: We use two of them $\mathbf{p}^{(1)} = [10^4, 10^4, 1]^T$ and $\mathbf{p}^{(2)} = [1, 1, 1]^T$ and

	$\mathbf{p}^{(1)}$	$\mathbf{p}^{(2)}$	$\mathbf{p}^{(3)}$	$\mathbf{p}^{(4)}$
p_1	10^4	1	10	10^4
p_2	10^4	1	10^4	10
p_3	1	1	1	1

Table 2: Example 6.2: parameter vectors (with $p_3 = 1$).

apply Algorithm 5.1 as follows: In step 2, we reduce the order of the systems to $r_1 = 8$ and $r_2 = 7$ using Algorithm 3.1, i.e. projection subspaces $\mathbf{V}^{(i)} \in \mathbb{R}^{4257\times r_i}$ and $\mathbf{W}^{(i)} \in \mathbb{R}^{4257\times r_i}$ were computed for $i = 1, 2$. We concatenate these matrices to build the final projection matrices

$$\mathbf{V}_r = [\mathbf{V}^{(1)},\ \mathbf{V}^{(2)}] \in \mathbb{R}^{4257\times15} \quad \text{and} \quad \mathbf{W}_r = [\mathbf{W}^{(1)},\ \mathbf{W}^{(2)}] \in \mathbb{R}^{4257\times15}.$$

Having removed the rank-deficient components from $\mathbf{V}_r$ and $\mathbf{W}_r$, our final parameterized reduced-order model is of order $r = 14$ and is given by

$$\mathbf{W}_r^T\mathbf{E}\mathbf{V}_r\dot{\mathbf{x}}_r(t) = (\mathbf{W}_r^T\mathbf{A}\mathbf{V}_r + \sum_{i=1}^{3} p_i\mathbf{W}_r^T\mathbf{A}_i\mathbf{V}_r)\mathbf{x}_r(t) + \mathbf{W}_r^T\mathbf{B}u(t), \quad \mathbf{y}_r(t) = \mathbf{C}\mathbf{V}_r\mathbf{x}_r(t).$$

To illustrate the quality of this reduced-order model, we fix $p_3 = 1$ and vary both p_1 and p_2 between 1 and 10^4. For each mesh point (i.e., for each triple of parameter values in this range), we compute the corresponding full-order model and the reduced-order model; and compute the corresponding relative $\mathcal{H}_\infty$ errors. The resulting mesh plot is given in Figure 11. The maximum relative $\mathcal{H}_\infty$ error is 2.16×10^{-2}. The parameterized reduced model $\mathbf{H}_r(s, \mathbf{p})$ has system order of less than 4% of the original system yet is able to maintain a small relative error of around 2% or less over the full range of variation of p_1 and p_2.

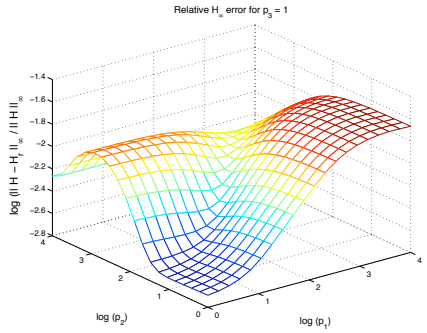

Figure 11: Example 6.2: relative $\mathcal{H}_\infty$ error as p_1 and p_2 vary.

6.2.1 Comparison with piecewise balanced truncation

As in the previous example, we present a comparison between our piecewise $\mathcal{H}_2$ optimal approach and piecewise balanced truncation that concatenates the projection matrices that are obtained by

Case:		A	B	C	D	E	F	G	H	I	J
dim. of proj. subsp. at $\mathbf{d}^{(i)}$	r_1	0	1	0	1	0	0	1	1	2	2
	r_2	1	1	0	0	1	0	0	1	2	2
	r_3	0	1	0	0	0	1	1	1	1	2
	r_4	1	1	2	2	2	2	2	2	2	2
	r_5	1	1	2	2	2	2	2	2	2	2
	r_6	1	1	2	2	2	2	2	2	2	2
Total dim r : $\mathbf{H}_r/\mathbf{H}_{\rm bal}$		4/4	6/6	5/5	7/7	7/7	7/7	7/7	8/7	9/9	12/12
Max. rel.	$\mathbf{H}_r$	2.85E-1	9.54E-2	1.21E-1	4.30E-2	4.65E-2	4.04E-2	3.91E-2	3.72E-2	5.23E-2	1.81E-2
$\mathcal{H}_\infty$-err.	$\mathbf{H}_{\rm bal}$	4.32E-2	∞	2.11E-2	2.26E-2	2.29E-2	2.57E-2	2.29E-2	2.51E-2	1.28E-2	∞
Max. rel.	$\mathbf{H}_r$	1.25E-1	7.79E-2	9.39E-2	4.23E-2	4.54E-2	3.94E-2	4.28E-2	2.43E-2	3.76E-2	1.49E-2
$\mathcal{H}_2$-err.	$\mathbf{H}_{\rm bal}$	9.89E-2	∞	3.91E-2	1.39E-1	1.28E-1	1.73E-1	1.41E-1	1.03E-1	1.27E-2	∞

Case:		K	L	M	N	O	P	Q	R	S	T
dim. of proj. subsp. at $\mathbf{d}^{(i)}$	r_1	1	1	1	1	2	0	1	1	2	3
	r_2	0	1	1	2	2	0	1	2	2	3
	r_3	0	0	1	1	2	0	1	2	3	3
	r_4	3	3	3	3	3	4	4	4	4	4
	r_5	3	3	3	3	3	4	4	4	4	4
	r_6	3	3	3	3	3	4	4	4	4	4
Total dim. r : $\mathbf{H}_r/\mathbf{H}_{\rm bal}$		10/10	10/11	11/12	12/13	14/13	12/12	14/15	16/16	16/16	17/17
Max. rel.	$\mathbf{H}_r$	7.66E-2	7.84E-2	7.64E-2	1.34E-2	1.16E-2	3.65E-2	1.46E-2	8.53E-3	2.12E-2	2.66E-3
$\mathcal{H}_\infty$-err.	$\mathbf{H}_{\rm bal}$	∞	∞	∞	∞	4.01E-2	1.41E-2	9.95E-3	1.74E-2	1.51E-3	6.10E-3
Max. rel.	$\mathbf{H}_r$	3.22E-2	3.23E-2	3.23E-2	6.54E-3	1.09E-2	1.74E-2	8.92E-3	4.46E-3	1.09E-2	2.13E-3
$\mathcal{H}_2$-err.	$\mathbf{H}_{\rm bal}$	∞	∞	∞	∞	2.19E-2	1.00E-2	4.91E-3	9.11E-3	8.05E-3	4.91E-3

Table 1: $\mathbf{H}_r$: Piecewise $\mathcal{H}_2$ optimal reduced model; $\mathbf{H}_{\rm bal}$: Piecewise balanced truncation reduced model

systems that are optimal $\mathcal{H}_2$ approximations to the original system. An optimal $\mathcal{H}_2$ approximant to the system $\mathbf{H}(s)$ is a system $\mathbf{H}_r(s)$ of reduced order, r, which solves:

$$\min_{\mathbf{H}_r \text{ is stable}} \|\mathbf{H}-\mathbf{H}_r\|_{\mathcal{H}_2}, \quad \text{where} \quad \|\mathbf{H}\|_{\mathcal{H}_2} := \left(\frac{1}{2\pi}\int_{-\infty}^{+\infty} \left\|\mathbf{H}(\imath\omega)\right\|_{\rm F}^2 d\omega\right)^{1/2},$$

and $\|\cdot\|_{\rm F}$ denotes the Frobenius norm of a matrix.

The set over which the optimization problem is posed, the set of all stable dynamical systems of order no greater than r, is nonconvex, so obtaining a global minimizer is at best a hard task and, indeed, it can be intractable. One moves instead toward a more modest goal and generally seeks "good" reduced models that satisfy first-order necessary optimality conditions, in principle allowing the possibility of having a local minimizer as an outcome. Many have worked on this problem; see [7, 29, 30, 35, 39, 41, 45, 46, 50]. Interpolation-based $\mathcal{H}_2$ optimality conditions were developed first by Meier and Luenberger [39] for SISO systems. Analogous $\mathcal{H}_2$ optimality conditions for MIMO systems have been placed within an interpolation framework recently in [10, 25, 43]. This is summarized in the next theorem:

Theorem 2. *Suppose $\widetilde{\mathbf{H}}_r(s) = \mathbf{C}_r(s\mathbf{E}_r - \mathbf{A}_r)^{-1}\mathbf{B}_r$ minimizes $\|\mathbf{H}-\mathbf{H}_r\|_{\mathcal{H}_2}$ over all (stable) rth-order transfer functions and that the associated reduced-order pencil $s\mathbf{E}_r - \mathbf{A}_r$ has distinct eigenvalues $\{\widetilde{\lambda}_i\}_{i=1}^r$. Let $\mathbf{y}_i^*$ and $\mathbf{x}_i$ denote left and right eigenvectors associated with $\widetilde{\lambda}_i$ so that $\mathbf{A}_r\mathbf{x}_i = \widetilde{\lambda}_i\mathbf{E}_r\mathbf{x}_i$, $\mathbf{y}_i^*\mathbf{A}_r = \widetilde{\lambda}_i\mathbf{y}_i^*\mathbf{E}_r$, and $\mathbf{y}_i^*\mathbf{E}_r\mathbf{x}_j = \delta_{ij}$. Define $\tilde{\mathbf{c}}_i = \mathbf{C}_r\mathbf{x}_i$ and $\tilde{\mathbf{b}}_i^T = \mathbf{y}_i^*\mathbf{B}_r$.*

Then the residue of $\widetilde{\mathbf{H}}_r(s)$ at $\widetilde{\lambda}_i$ is matrix-valued and has rank one: $\mathrm{res}[\widetilde{\mathbf{H}}_r(s), \widetilde{\lambda}_i] = \tilde{\mathbf{c}}_i\tilde{\mathbf{b}}_i^T$. *We can write $\widetilde{\mathbf{H}}_r(s) = \sum_{i=1}^r \frac{1}{s-\widetilde{\lambda}_i}\tilde{\mathbf{c}}_i\tilde{\mathbf{b}}_i^T$. Then, for $i = 1, \cdots, r$,*

$$\mathbf{H}(-\widetilde{\lambda}_i)\tilde{\mathbf{b}}_i = \widetilde{\mathbf{H}}_r(-\widetilde{\lambda}_i)\tilde{\mathbf{b}}_i, \quad \tilde{\mathbf{c}}_i^T\mathbf{H}(-\widetilde{\lambda}_i) = \tilde{\mathbf{c}}_i^T\widetilde{\mathbf{H}}_r(-\widetilde{\lambda}_i),$$
$$\text{and} \quad \tilde{\mathbf{c}}_i^T\mathbf{H}'(-\widetilde{\lambda}_i)\tilde{\mathbf{b}}_i = \tilde{\mathbf{c}}_i^T\widetilde{\mathbf{H}}_r'(-\widetilde{\lambda}_i)\tilde{\mathbf{b}}_i. \tag{14}$$

That is, first-order conditions for $\mathcal{H}_2$ optimality can be formulated as tangential interpolation conditions at reflected images of $\widetilde{\lambda}_i$ through the origin.

Evidently, the $\mathcal{H}_2$ optimal interpolation points and associated tangent directions depend on knowledge of the reduced-order system and so will not be available *a priori*. An iterative algorithm was introduced in [25], called the *Iterative Rational Krylov Algorithm* (IRKA), built on successive substitution. Interpolation points used for the next step are chosen to be the reflected images of reduced-order poles for the current step: $\sigma \leftarrow -\widetilde{\lambda}$ for eigenvalues, $\widetilde{\lambda}_i$, of the pencil $\lambda\mathbf{E}_r - \mathbf{A}_r$ associated with reduced matrices of the current step. The tangent directions are corrected in a similar way, using residues of the previous reduced model successively until (14) is satisfied. A brief sketch of IRKA is described in Algorithm 3.1.

From Steps 3.*d* and 3.*e*, one sees that upon convergence, the reduced transfer function will satisfy, (14), first-order conditions for $\mathcal{H}_2$ optimality. The main computational cost involves solving $2r$ linear systems at every step to generate $\mathbf{V}_r$ and $\mathbf{W}_r$. Computing the left and right eigenvectors $\mathbf{y}_i$ and $\mathbf{x}_i$, and eigenvalues, $\lambda_i(\mathbf{A}_r, \mathbf{E}_r)$, of the reduced pencil $\lambda\mathbf{E}_r - \mathbf{A}_r$ is cheap since the dimension r is small.

4 Interpolatory Model Reduction of Parameterized Systems

We are able to extend the results of the previous section in a natural way to an interpolation framework for applying PMOR to the parameterized system (1)–(2) in order to produce a parameterized reduced system (3)–(4). In addition to the basic interpolation conditions for the transfer function as in (14), we develop conditions that also will guarantee matching of both the gradient and Hessian of the transfer function *with respect to the parameters*. Our framework allows parameter dependency (linear or nonlinear) in all state-space quantities.

Algorithm 3.1. MIMO $\mathcal{H}_2$ optimal tangential interpolation method

1. *Make an initial r-fold shift selection: $\{\sigma_1, \ldots, \sigma_r\}$ that is closed under conjugation (i.e., $\{\sigma_1, \ldots, \sigma_r\} \equiv \{\overline{\sigma_1}, \ldots, \overline{\sigma_r}\}$ viewed as sets)*
   and initial tangent directions $\widetilde{\mathbf{b}}_1, \ldots, \widetilde{\mathbf{b}}_r$ and $\widetilde{\mathbf{c}}_1, \ldots, \widetilde{\mathbf{c}}_r$, also closed under conjugation.
2. $\mathbf{V}_r = \left[(\sigma_1 \mathbf{E} - \mathbf{A})^{-1} \mathbf{B} \widetilde{\mathbf{b}}_1 , \ldots, (\sigma_r \mathbf{E} - \mathbf{A})^{-1} \mathbf{B} \widetilde{\mathbf{b}}_r \right]$,
   $\mathbf{W}_r^T = \left[\left(\widetilde{\mathbf{c}}_1^T \mathbf{C} (\sigma_1 \mathbf{E} - \mathbf{A})^{-1} \right)^T , \ldots, \left(\widetilde{\mathbf{c}}_r^T \mathbf{C} (\sigma_r \mathbf{E} - \mathbf{A})^{-1} \right)^T \right]^T$.
3. *while (not converged)*
   a) $\mathbf{A}_r = \mathbf{W}_r^T \mathbf{A} \mathbf{V}_r$, $\mathbf{E}_r = \mathbf{W}_r^T \mathbf{E} \mathbf{V}_r$, $\mathbf{B}_r = \mathbf{W}_r^T \mathbf{B}$, *and* $\mathbf{C}_r = \mathbf{C} \mathbf{V}_r$.
   b) *Compute* $\mathbf{A}_r \mathbf{x}_i = \tilde{\lambda}_i \mathbf{E}_r \mathbf{x}_i$ *and* $\mathbf{y}_i^* \mathbf{A}_r = \tilde{\lambda}_i \mathbf{y}_i^* \mathbf{E}_r$ *with* $\mathbf{y}_i^* \mathbf{E}_r \mathbf{x}_j = \delta_{ij}$ *where* $\mathbf{y}_i^*$ *and* $\mathbf{x}_i$ *are left and right eigenvectors associated with* $\tilde{\lambda}_i$.
   c) $\sigma_i \leftarrow -\tilde{\lambda}_i$, $\widetilde{\mathbf{b}}_i^T \leftarrow \mathbf{y}_i^* \mathbf{B}_r$ *and* $\widetilde{\mathbf{c}}_i \leftarrow \mathbf{C}_r \mathbf{x}_i$, *for* $i = 1, \ldots, r$.
   d) $\mathbf{V}_r = \left[(\sigma_1 \mathbf{E} - \mathbf{A})^{-1} \mathbf{B} \widetilde{\mathbf{b}}_1 , \ldots, (\sigma_r \mathbf{E} - \mathbf{A})^{-1} \mathbf{B} \widetilde{\mathbf{b}}_r \right]$.
   e) $\mathbf{W}_r^T = \left[\left(\widetilde{\mathbf{c}}_1^T \mathbf{C} (\sigma_1 \mathbf{E} - \mathbf{A})^{-1} \right)^T , \ldots, \left(\widetilde{\mathbf{c}}_r^T \mathbf{C} (\sigma_r \mathbf{E} - \mathbf{A})^{-1} \right)^T \right]^T$.
4. $\mathbf{A}_r = \mathbf{W}_r^T \mathbf{A} \mathbf{V}_r$, $\mathbf{E}_r = \mathbf{W}_r^T \mathbf{E} \mathbf{V}_r$, $\mathbf{B}_r = \mathbf{W}_r^T \mathbf{B}$, $\mathbf{C}_r = \mathbf{C} \mathbf{V}_r$.

Theorem 3. *Suppose $\sigma \in \mathbb{C}$ and $\hat{\mathbf{p}} \in \mathbb{C}^\nu$ is such that both $\sigma \mathbf{E}(\hat{\mathbf{p}}) - \mathbf{A}(\hat{\mathbf{p}})$ and $\sigma \mathbf{E}_r(\hat{\mathbf{p}}) - \mathbf{A}_r(\hat{\mathbf{p}})$ are invertible. Suppose $\mathbf{b} \in \mathbb{C}^m$ and $\mathbf{c} \in \mathbb{C}^\ell$ are fixed nontrivial vectors.*

a) If $(\sigma \mathbf{E}(\hat{\mathbf{p}}) - \mathbf{A}(\hat{\mathbf{p}}))^{-1} \mathbf{B}(\hat{\mathbf{p}}) \mathbf{b} \in \mathrm{Ran}(\mathbf{V}_r)$, *then* $\mathbf{H}(\sigma, \hat{\mathbf{p}}) \mathbf{b} = \mathbf{H}_r(\sigma, \hat{\mathbf{p}}) \mathbf{b}$. (15)

b) If $\left(\mathbf{c}^T \mathbf{C}(\hat{\mathbf{p}}) (\sigma \mathbf{E}(\hat{\mathbf{p}}) - \mathbf{A}(\hat{\mathbf{p}}))^{-1} \right)^T \in \mathrm{Ran}(\mathbf{W}_r)$, *then* $\mathbf{c}^T \mathbf{H}(\sigma, \hat{\mathbf{p}}) = \mathbf{c}^T \mathbf{H}_r(\sigma, \hat{\mathbf{p}})$. (16)

Proof. Define $\boldsymbol{\mathcal{A}}(s, \mathbf{p}) = s\mathbf{E}(\mathbf{p}) - \mathbf{A}(\mathbf{p})$ and $\boldsymbol{\mathcal{A}}_r(s, \mathbf{p}) = s\mathbf{E}_r(\mathbf{p}) - \mathbf{A}_r(\mathbf{p}) = \mathbf{W}_r^T \boldsymbol{\mathcal{A}}(s, \mathbf{p}) \mathbf{V}_r$, and consider the (skew) projections

$$\boldsymbol{\mathcal{P}}_r(s, \mathbf{p}) = \mathbf{V}_r \boldsymbol{\mathcal{A}}_r(s, \mathbf{p})^{-1} \mathbf{W}_r^T \boldsymbol{\mathcal{A}}(s, \mathbf{p}) \quad \text{and} \quad \boldsymbol{\Omega}_r(s, \mathbf{p}) = \boldsymbol{\mathcal{A}}(s, \mathbf{p}) \mathbf{V}_r \boldsymbol{\mathcal{A}}_r(s, \mathbf{p})^{-1} \mathbf{W}_r^T.$$

Define $\mathbf{f}(s, \mathbf{p}) = \boldsymbol{\mathcal{A}}(s, \mathbf{p})^{-1} \mathbf{B}(\mathbf{p}) \mathbf{b}$ and $\mathbf{g}^T(s, \mathbf{p}) = \mathbf{c}^T \mathbf{C}(\mathbf{p}) \boldsymbol{\mathcal{A}}(s, \mathbf{p})^{-1}$. Then observe that the hypotheses of (15) means $\mathbf{f}(\sigma, \hat{\mathbf{p}}) \in \mathrm{Ran}(\boldsymbol{\mathcal{P}}_r(\sigma, \hat{\mathbf{p}}))$ and thus

$$\mathbf{H}(\sigma, \hat{\mathbf{p}}) \mathbf{b} - \mathbf{H}_r(\sigma, \hat{\mathbf{p}}) \mathbf{b} = \mathbf{C}(\hat{\mathbf{p}}) \left(\mathbf{I} - \boldsymbol{\mathcal{P}}_r(\sigma, \hat{\mathbf{p}}) \right) \mathbf{f}(\sigma, \hat{\mathbf{p}}) = 0,$$

proving (a). Analogously, the hypotheses of (16) means $\mathbf{g}(\sigma, \hat{\mathbf{p}}) \perp \mathrm{Ker}(\boldsymbol{\Omega}_r(\sigma, \hat{\mathbf{p}}))$ and

$$\mathbf{c}^T \mathbf{H}(\sigma, \hat{\mathbf{p}}) - \mathbf{c}^T \mathbf{H}_r(\sigma, \hat{\mathbf{p}}) = \mathbf{g}^T(\sigma, \hat{\mathbf{p}}) \left(\mathbf{I} - \boldsymbol{\Omega}_r(\sigma, \hat{\mathbf{p}}) \right) \mathbf{B}(\hat{\mathbf{p}}) = 0,$$

yielding (b). □

Next, we show how to construct an interpolatory reduced-order model whose transfer function not only interpolates the original one, but also matches its gradient with respect to the given parameter set.

Theorem 4. *Assume the hypotheses of Theorem 3. Suppose, in addition, that* $\mathbf{E}(\mathbf{p})$, $\mathbf{A}(\mathbf{p})$, $\mathbf{B}(\mathbf{p})$, *and* $\mathbf{C}(\mathbf{p})$ *are continuously differentiable in a neighborhood of* $\hat{\mathbf{p}}$. *Then both* $\mathbf{c}^T \mathbf{H}(\sigma, \mathbf{p}) \mathbf{b}$ *and*

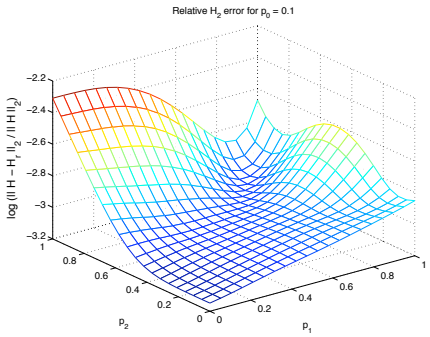

Figure 9: Example 6.1 ($\nu = 3$) with piecewise balanced truncation: relative $\mathcal{H}_2$ error.

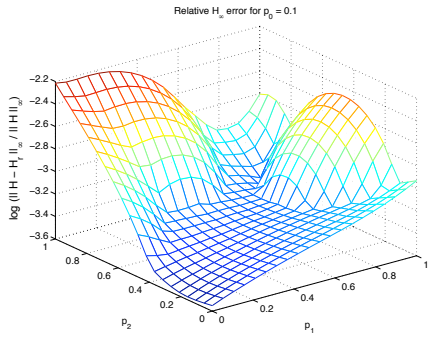

Figure 10: Example 6.1 ($\nu = 3$) with piecewise balanced truncation: relative $\mathcal{H}_\infty$ error.

models. Note that in another PMOR approach based on balanced truncation and interpolation [3] the computation of unstable systems is avoided.

6.2 Thermal conduction in a semiconductor chip

We consider now a model representing thermal conduction in a semiconductor chip as described in [34]. An important requirement for a compact and efficient model of thermal conduction in this context is that it should allow flexibility in specifying boundary conditions in order to allow independent designers to evaluate how changes in the environment can influence the temperature distribution in the chip. The thermal problem is modeled as homogenous heat diffusion with heat exchange occurring at three device interfaces modeled with convection boundary conditions. These conditions introduce film coefficients, p_1, p_2, and p_3, describing the heat exchange on the three device interfaces. Discretization leads to a system of ordinary differential equations

$$\mathbf{E}\dot{\mathbf{x}}(t) = (\mathbf{A} + \sum_{i=1}^{3} p_i \mathbf{A}_i)\mathbf{x}(t) + \mathbf{B}u(t), \quad \mathbf{y}(t) = \mathbf{C}\mathbf{x}(t),$$

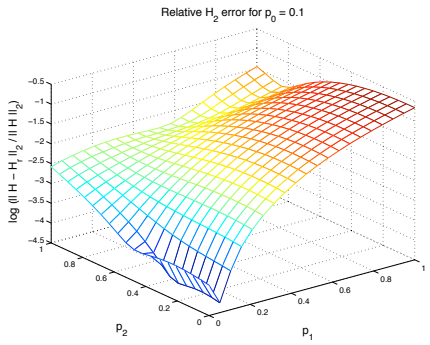

Figure 7: Example 6.1 ($\nu = 3$) without optimal $\mathcal{H}_2$ shift selection: relative $\mathcal{H}_2$ error.

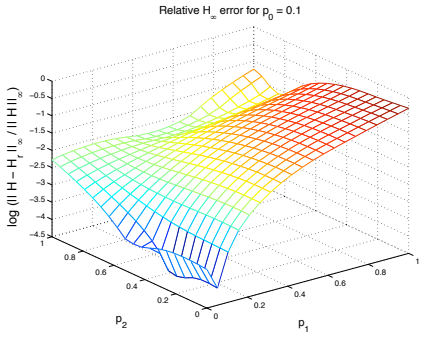

Figure 8: Example 6.1 ($\nu = 3$) without optimal $\mathcal{H}_2$ shift selection: relative $\mathcal{H}_\infty$ error.

$\mathbf{p}^{(i)}$. On the other hand, if $\mathbf{V}^{(i)}$ and $\mathbf{W}^{(i)}$ are interpolating spaces that are obtained by forcing interpolation at some interpolation points $\{\sigma_{ik}\}_{k=1}^{r_i}$ for the parameter set described by $\mathbf{p}^{(i)}$, even after the subspaces are concatenated, the final reduced-order parameterized model would still interpolate the original model at the same interpolation points $\{\sigma_{ik}\}_{k=1}^{r_i}$ for the parameter set $\mathbf{p}^{(i)}$. In short, our piecewise $\mathcal{H}_2$ optimal algorithm has two important properties. Firstly, due to the interpolatory structure, the final parameterized reduced-order model interpolates the original one even after the subspaces augmented. Secondly, the interpolation points at each parameter set are chosen in an $\mathcal{H}_2$ optimal way yielding accurate reduced-order models.

To more thoroughly compare the two approaches, we used many different values for $r_1, r_2, \ldots, r_6$ at the corresponding parameter values $\mathbf{p}^{(i)}$ and computed the corresponding reduced-order models both by balanced truncation and by IRKA, producing projection subspaces $\mathbf{V}^{(i)}$ and $\mathbf{W}^{(i)}$. The final reduced-order parameterized systems are obtained as in (3) and their quality is compared by computing the maximum relative $\mathcal{H}_2$ error and $\mathcal{H}_\infty$ error again varying p_1 and p_2 over the full parameter range of [0, 1]. The results are tabulated in Table 1. In this table, the ∞ entries indicate that some unstable reduced-order models were encountered for some choices of p_1 and p_2. The table shows that except for cases where the approach using balanced truncation results in unstable reduced-order models, both approaches are comparable yielding similar quality reduced-order

$\mathbf{c}^T\mathbf{H}_r(\sigma,\mathbf{p})\mathbf{b}$ *are differentiable with respect to* $\mathbf{p}$ *in a neighborhood of* $\hat{\mathbf{p}}$ *as well.*

$$\begin{aligned} &\textit{If both } \left(\sigma\,\mathbf{E}(\hat{\mathbf{p}}) - \mathbf{A}(\hat{\mathbf{p}})\right)^{-1}\mathbf{B}(\hat{\mathbf{p}})\mathbf{b} \in \mathrm{Ran}(\mathbf{V}_r) \\ &\quad \textit{and } \left(\mathbf{c}^T\mathbf{C}(\hat{\mathbf{p}})\left(\sigma\,\mathbf{E}(\hat{\mathbf{p}}) - \mathbf{A}(\hat{\mathbf{p}})\right)^{-1}\right)^T \in \mathrm{Ran}(\mathbf{W}_r), \end{aligned} \tag{17}$$

$$\textit{then } \nabla_{\mathbf{p}}\mathbf{c}^T\mathbf{H}(\sigma,\hat{\mathbf{p}})\mathbf{b} = \nabla_{\mathbf{p}}\mathbf{c}^T\mathbf{H}_r(\sigma,\hat{\mathbf{p}})\mathbf{b}. \tag{18}$$

From Theorem 1, these conditions also guarantee $\frac{\partial}{\partial s}\mathbf{c}^T\mathbf{H}(\sigma,\hat{\mathbf{p}})\mathbf{b} = \frac{\partial}{\partial s}\mathbf{c}^T\mathbf{H}_r(\sigma,\hat{\mathbf{p}})\mathbf{b}$.

Proof. Fix an arbitrary nontrivial direction $\mathbf{n} = [n_1, \ldots, n_\nu]^T \in \mathbb{C}^\nu$ and denote the associated directional derivative as

$$\mathbf{n}\cdot\nabla_{\mathbf{p}} = \sum_{i=1}^{\nu} n_i \frac{\partial}{\partial p_i}.$$

Note that for all s and $\mathbf{p}$ at which $\mathcal{P}_r$ and $\mathcal{Q}_r$ are continuous, we have:
$\mathrm{Ran}\left((\mathbf{n}\cdot\nabla_{\mathbf{p}})\mathcal{P}_r(s,\mathbf{p})\right) \subset \mathrm{Ran}\left(\mathcal{P}_r(s,\mathbf{p})\right)$ and $\mathrm{Ker}\left((\mathbf{n}\cdot\nabla_{\mathbf{p}})\mathcal{Q}_r(s,\mathbf{p})\right) \supset \mathrm{Ker}\left(\mathcal{Q}_r(s,\mathbf{p})\right)$. Thus

$$\left(\mathbf{I}-\mathcal{P}_r(s,\mathbf{p})\right)\left[(\mathbf{n}\cdot\nabla_{\mathbf{p}})\mathcal{P}_r(s,\mathbf{p})\right] = 0 \text{ and } \left[(\mathbf{n}\cdot\nabla_{\mathbf{p}})\mathcal{Q}_r(s,\mathbf{p})\right]\left(\mathbf{I}-\mathcal{Q}_r(s,\mathbf{p})\right) = 0. \tag{19}$$

As a consequence,

$$(\mathbf{n}\cdot\nabla_{\mathbf{p}})\left[\left(\mathbf{I}-\mathcal{Q}_r(s,\mathbf{p})\right)\mathcal{A}(s,\mathbf{p})\left(\mathbf{I}-\mathcal{P}_r(s,\mathbf{p})\right)\right] = \left(\mathbf{I}-\mathcal{Q}_r(s,\mathbf{p})\right)\left[(\mathbf{n}\cdot\nabla_{\mathbf{p}})\mathcal{A}(s,\mathbf{p})\right]\left(\mathbf{I}-\mathcal{P}_r(s,\mathbf{p})\right).$$

Observe that

$$\mathbf{c}^T\mathbf{H}(s,\mathbf{p})\mathbf{b} - \mathbf{c}^T\mathbf{H}_r(s,\mathbf{p})\mathbf{b} = \mathbf{g}^T(s,\mathbf{p})\left(\mathbf{I}-\mathcal{Q}_r(s,\mathbf{p})\right)\mathcal{A}(s,\mathbf{p})\left(\mathbf{I}-\mathcal{P}_r(s,\mathbf{p})\right)\mathbf{f}(s,\mathbf{p}).$$

So, we may calculate a directional derivative and evaluate at $s=\sigma$ and $\mathbf{p}=\hat{\mathbf{p}}$:

$$\begin{aligned} &(\mathbf{n}\cdot\nabla_{\mathbf{p}})\left[\mathbf{c}^T\mathbf{H}(\sigma,\mathbf{p})\mathbf{b} - \mathbf{c}^T\mathbf{H}_r(\sigma,\mathbf{p})\mathbf{b}\right]\big|_{\mathbf{p}=\hat{\mathbf{p}}} = \\ &\quad \left[(\mathbf{n}\cdot\nabla_{\mathbf{p}})\mathbf{g}^T(\sigma,\hat{\mathbf{p}})\right]\left(\mathbf{I}-\mathcal{Q}_r(\sigma,\hat{\mathbf{p}})\right)\mathcal{A}(\sigma,\hat{\mathbf{p}})\left(\mathbf{I}-\mathcal{P}_r(\sigma,\hat{\mathbf{p}})\right)\mathbf{f}(\sigma,\hat{\mathbf{p}}) \\ &\qquad + \mathbf{g}^T(\sigma,\hat{\mathbf{p}})\left(\mathbf{I}-\mathcal{Q}_r(\sigma,\hat{\mathbf{p}})\right)\left[(\mathbf{n}\cdot\nabla_{\mathbf{p}})\mathcal{A}(\sigma,\hat{\mathbf{p}})\right]\left(\mathbf{I}-\mathcal{P}_r(\sigma,\hat{\mathbf{p}})\right)\mathbf{f}(\sigma,\hat{\mathbf{p}}) \\ &\qquad\quad + \mathbf{g}^T(\sigma,\hat{\mathbf{p}})\left(\mathbf{I}-\mathcal{Q}_r(\sigma,\hat{\mathbf{p}})\right)\mathcal{A}(\sigma,\hat{\mathbf{p}})\left(\mathbf{I}-\mathcal{P}_r(\sigma,\hat{\mathbf{p}})\right)\left[(\mathbf{n}\cdot\nabla_{\mathbf{p}})\mathbf{f}(\sigma,\hat{\mathbf{p}})\right]. \end{aligned}$$

The hypotheses (17) implies both $\mathbf{f}(\sigma,\hat{\mathbf{p}}) \in \mathrm{Ran}(\mathcal{P}_r(\sigma,\hat{\mathbf{p}}))$ and $\mathbf{g}(\sigma,\hat{\mathbf{p}}) \perp \mathrm{Ker}(\mathcal{Q}_r(\sigma,\hat{\mathbf{p}}))$ so $(\mathbf{n}\cdot\nabla_{\mathbf{p}})\left[\mathbf{c}^T\mathbf{H}(\sigma,\mathbf{p})\mathbf{b} - \mathbf{c}^T\mathbf{H}_r(\sigma,\mathbf{p})\mathbf{b}\right]\big|_{\mathbf{p}=\hat{\mathbf{p}}} = 0$. Since $\mathbf{n}$ was arbitrarily chosen the conclusion follows. □

Notice that the conditions (17) of Theorem 4 are enforced as a matter of course (for the nonparameterized case) in Algorithm 3.1. For SISO systems (where tangent directions play no role), we create a parameterized reduced system, $H_r(s,\mathbf{p})$, that is not only a Hermite interpolant (with respect to frequency) to $H(s,\mathbf{p})$ at $(\sigma,\hat{\mathbf{p}})$ but the $\mathbf{p}$-*gradients* of H_r and H will also match at $(\sigma,\hat{\mathbf{p}})$ and we can guarantee this matching for essentially no greater cost without computing the $\mathbf{p}$-gradient of either $H_r(s,\mathbf{p})$ or $H(s,\mathbf{p})$. This is a significant feature with regard to sensitivity analysis [11]: notice that the parameterized reduced-order model may be used to compute parameter sensitivities more cheaply than the original model and will exactly match the original model sensitivities at every parameter interpolation point, $\hat{\mathbf{p}}$.

There are also interesting consequences for optimization with respect to $\mathbf{p}$ of objective functions depending on $\mathbf{H}(s,\mathbf{p})$ (or on the output $\widehat{\mathbf{y}}(s,\mathbf{p})$ for a fixed input $\widehat{\mathbf{u}}$). Under natural auxiliary conditions, reduced-order models satisfying the conditions (17) of Theorem 4 will lead to, in the terminology of [1], *first order accurate approximate models* for the objective function and this feature is sufficient in establishing robust convergence behaviour of related trust region methods utilizing reduced-order models as surrogate models.

In the context of optimization, the next obvious question is under what conditions will a reduced-order model retain the same *curvature* or *Hessian* information with respect to parameters as the original model ?

Theorem 5. *Assume the hypotheses of Theorem 4 including (17) and suppose that* $\mathbf{E}(\mathbf{p})$, $\mathbf{A}(\mathbf{p})$, $\mathbf{B}(\mathbf{p})$, *and* $\mathbf{C}(\mathbf{p})$ *are twice continuously differentiable in a neighborhood of* $\hat{\mathbf{p}}$. *Then* $\mathbf{c}^T\mathbf{H}(\sigma,\mathbf{p})\mathbf{b}$ *and* $\mathbf{c}^T\mathbf{H}_r(\sigma,\mathbf{p})\mathbf{b}$ *are each twice continuously differentiable at* $\hat{\mathbf{p}}$.

a) Let $\{\mathbf{n}_1, \mathbf{n}_2, \ldots, \mathbf{n}_\nu\}$ *be a basis for* $\mathbb{C}^\nu$ *with related quantities*

$$\mathbf{f}_i(\sigma,\hat{\mathbf{p}}) = \left(\mathbf{n}_i \cdot \nabla_{\mathbf{p}}\right)(\sigma\,\mathbf{E}(\hat{\mathbf{p}}) - \mathbf{A}(\hat{\mathbf{p}}))^{-1}\mathbf{B}(\hat{\mathbf{p}})\mathbf{b} \quad \textit{and}$$
$$\mathbf{g}_i^T(\sigma,\hat{\mathbf{p}}) = \left(\mathbf{n}_i \cdot \nabla_{\mathbf{p}}\right)\mathbf{c}^T\mathbf{C}(\hat{\mathbf{p}})\left(\sigma\,\mathbf{E}(\hat{\mathbf{p}}) - \mathbf{A}(\hat{\mathbf{p}})\right)^{-1}.$$

$$\textit{If either } \{\mathbf{f}_1, \mathbf{f}_2, \ldots, \mathbf{f}_\nu\} \subset \mathrm{Ran}(\mathbf{V}_r) \tag{20}$$
$$\textit{or } \{\mathbf{g}_1, \mathbf{g}_2, \ldots, \mathbf{g}_\nu\} \subset \mathrm{Ran}(\mathbf{W}_r), \tag{21}$$
$$\textit{then } \nabla^2_{\mathbf{p}}[\mathbf{c}^T\mathbf{H}(\sigma,\hat{\mathbf{p}})\mathbf{b}] = \nabla^2_{\mathbf{p}}[\mathbf{c}^T\mathbf{H}_r(\sigma,\hat{\mathbf{p}})\mathbf{b}].$$

b) Let $\mathbf{n}$ *be a fixed nontrivial vector in* $\mathbb{C}^\nu$ *and suppose that*

$$\left(\mathbf{n} \cdot \nabla_{\mathbf{p}}\right)(\sigma\,\mathbf{E}(\hat{\mathbf{p}}) - \mathbf{A}(\hat{\mathbf{p}}))^{-1}\,\mathbf{B}(\hat{\mathbf{p}})\mathbf{b} \in \mathrm{Ran}(\mathbf{V}_r) \textit{ and}$$
$$\left(\mathbf{n} \cdot \nabla_{\mathbf{p}}\right)\left(\mathbf{c}^T\mathbf{C}(\hat{\mathbf{p}})\left(\sigma\,\mathbf{E}(\hat{\mathbf{p}}) - \mathbf{A}(\hat{\mathbf{p}})\right)^{-1}\right)^T \in \mathrm{Ran}(\mathbf{W}_r).$$

$$\textit{Then} \quad \nabla^2_{\mathbf{p}}[\mathbf{c}^T\mathbf{H}(\sigma,\hat{\mathbf{p}})\mathbf{b}]\,\mathbf{n} = \nabla^2_{\mathbf{p}}[\mathbf{c}^T\mathbf{H}_r(\sigma,\hat{\mathbf{p}})\mathbf{b}]\,\mathbf{n}. \tag{22}$$

Proof. Let $\mathbf{n} = [n_1, \ldots, n_\nu]^T$ and $\mathbf{m} = [m_1, \ldots, m_\nu]^T$ be arbitrary vectors in $\mathbb{C}^\nu$ and consider the composition of the associated directional derivatives:

$$(\mathbf{m} \cdot \nabla_{\mathbf{p}})(\mathbf{n} \cdot \nabla_{\mathbf{p}})\left[\mathbf{c}^T\mathbf{H}(\sigma,\mathbf{p})\mathbf{b} - \mathbf{c}^T\mathbf{H}_r(\sigma,\mathbf{p})\mathbf{b}\right]\Big|_{\mathbf{p}=\hat{\mathbf{p}}} = \mathbf{m}^T\,\nabla^2_{\mathbf{p}}[\mathbf{c}^T\mathbf{H}(\sigma,\hat{\mathbf{p}})\mathbf{b} - \mathbf{c}^T\mathbf{H}_r(\sigma,\hat{\mathbf{p}})\mathbf{b}]\,\mathbf{n}.$$

Using (19), one may calculate:

$$\begin{aligned}(\mathbf{m} \cdot \nabla_{\mathbf{p}})(\mathbf{n} \cdot \nabla_{\mathbf{p}})\left[(\mathbf{I} - \mathcal{Q}_r(s,\mathbf{p}))\,\mathcal{A}(s,\mathbf{p})\,(\mathbf{I} - \mathcal{P}_r(s,\mathbf{p}))\right] = \\ - \left[(\mathbf{m} \cdot \nabla_{\mathbf{p}})\mathcal{Q}_r(s,\mathbf{p})\right]\left[(\mathbf{n} \cdot \nabla_{\mathbf{p}})\mathcal{A}(s,\mathbf{p})\right](\mathbf{I} - \mathcal{P}_r(s,\mathbf{p})) \\ + (\mathbf{I} - \mathcal{Q}_r(s,\mathbf{p}))\left[(\mathbf{m} \cdot \nabla_{\mathbf{p}})(\mathbf{n} \cdot \nabla_{\mathbf{p}})\mathcal{A}(s,\mathbf{p})\right](\mathbf{I} - \mathcal{P}_r(s,\mathbf{p})) \\ - (\mathbf{I} - \mathcal{Q}_r(s,\mathbf{p}))\left[(\mathbf{n} \cdot \nabla_{\mathbf{p}})\mathcal{A}(s,\mathbf{p})\right]\left[(\mathbf{m} \cdot \nabla_{\mathbf{p}})\mathcal{P}_r(s,\mathbf{p})\right].\end{aligned}$$

Then with (17), one finds

$$\begin{aligned}\mathbf{m}^T\,\nabla^2_{\mathbf{p}}[\mathbf{c}^T\mathbf{H}(\sigma,\hat{\mathbf{p}})\mathbf{b} - \mathbf{c}^T\mathbf{H}_r(\sigma,\hat{\mathbf{p}})\mathbf{b}]\,\mathbf{n} = \\ \Big[\left[(\mathbf{m} \cdot \nabla_{\mathbf{p}})\mathbf{c}^T\mathbf{C}(\mathbf{p})\mathcal{A}(s,\mathbf{p})^{-1}\right] \cdot (\mathbf{I} - \mathcal{Q}_r(s,\mathbf{p}))\,\mathcal{A}(s,\mathbf{p})\,(\mathbf{I} - \mathcal{P}_r(s,\mathbf{p})) \cdot \\ \left[(\mathbf{n} \cdot \nabla_{\mathbf{p}})\mathcal{A}(s,\mathbf{p})^{-1}\mathbf{B}(\mathbf{p})\mathbf{b}\right] \\ + \left[(\mathbf{n} \cdot \nabla_{\mathbf{p}})\mathbf{c}^T\mathbf{C}(\mathbf{p})\mathcal{A}(s,\mathbf{p})^{-1}\right] \cdot (\mathbf{I} - \mathcal{Q}_r(s,\mathbf{p}))\,\mathcal{A}(s,\mathbf{p})\,(\mathbf{I} - \mathcal{P}_r(s,\mathbf{p})) \cdot \\ \left[(\mathbf{m} \cdot \nabla_{\mathbf{p}})\mathcal{A}(s,\mathbf{p})^{-1}\mathbf{B}(\mathbf{p})\mathbf{b}\right]\Big]\Big|_{\mathbf{p}=\hat{\mathbf{p}}}.\end{aligned}$$

If (20) holds then both vectors $(\mathbf{m} \cdot \nabla_{\mathbf{p}})\mathcal{A}(s,\hat{\mathbf{p}})^{-1}\mathbf{B}(\hat{\mathbf{p}})\mathbf{b}$ and $(\mathbf{n} \cdot \nabla_{\mathbf{p}})\mathcal{A}(s,\hat{\mathbf{p}})^{-1}\mathbf{B}(\hat{\mathbf{p}})\mathbf{b}$ are in $\mathrm{Ran}(\mathcal{P}_r(\sigma,\hat{\mathbf{p}}))$, leading to the conclusion of (a), since $\mathbf{m}$ and $\mathbf{n}$ could be arbitrarily chosen. A similar argument holds if (21) is true.

If the hypotheses of (b) holds then observe that

$$\mathbf{m}^T\,\nabla^2_{\mathbf{p}}[\mathbf{c}^T\mathbf{H}(\sigma,\hat{\mathbf{p}})\mathbf{b} - \mathbf{c}^T\mathbf{H}_r(\sigma,\hat{\mathbf{p}})\mathbf{b}]\,\mathbf{n} = 0,$$

independent of how $\mathbf{m}$ is chosen, which then yields the conclusion (22). □

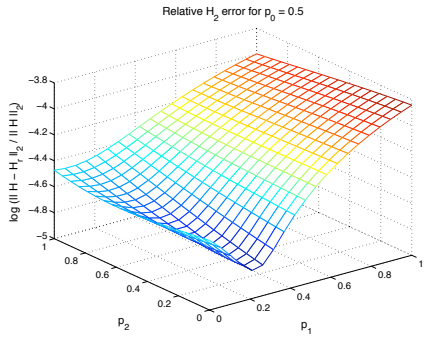

Figure 5: Example 6.1 with $\nu = 3$: relative $\mathcal{H}_2$ error as p_1 and p_2 vary.

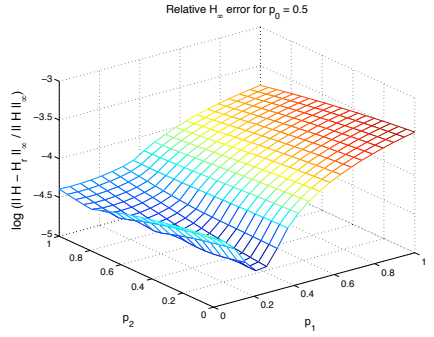

Figure 6: Example 6.1 with $\nu = 3$: relative $\mathcal{H}_\infty$ error for as p_1 and p_2 vary.

adjusted these points iteratively without any user intervention, yielding in the end very accurate parameterized reduced models. Since the IRKA iteration generally converges very quickly (see [25]), the additional sparse linear systems that must be solved do not significantly increase cost, yet additional iterations increase the accuracy of the reduced model by two orders of magnitude.

Next, we compare our piecewise $\mathcal{H}_2$ optimal method with an approach where *balanced truncation* is used to reduce the order at each parameter set, $\mathbf{p}^{(i)}$. Towards this goal, we chose a reduced order of four at each parameter value and obtained corresponding $\mathbf{V}^{(i)}$ and $\mathbf{W}^{(i)}$ for $i = 1, \ldots, 6$. Then as before, we concatenate the subspaces obtained by balanced truncation to form a final parameterized reduced-order model; since it is similar in structure to our piecewise $\mathcal{H}_2$ optimal method, we call this "piecewise balanced truncation". (Note that this approach differs from the hybrid interpolation balanced truncation method described in [3].) For a fixed $p_0 = 0.1$, the maximum relative $\mathcal{H}_\infty$ error calculated on the same grid for p_1 and p_2 is 6.10×10^{-3}; the maximum relative $\mathcal{H}_2$ error 4.91×10^{-3}. Plots for the relative $\mathcal{H}_2$ error and relative $\mathcal{H}_\infty$ error are shown in Figures 9 and 10, respectively. We note that both errors are somewhat higher than the results obtained by the proposed approach in Section 5. This result is not surprising. Even though $\mathbf{V}^{(i)}$ and $\mathbf{W}^{(i)}$ are the balancing subspaces at the parameter values $\mathbf{p}^{(i)}$, once they are concatenated, the resulting reduced-order model is *no longer* balanced even when evaluated at the parameter set

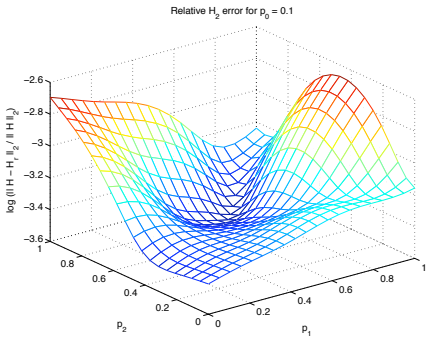

Figure 3: Example 6.1 with $\nu = 3$: relative $\mathcal{H}_2$ error as p_1 and p_2 vary.

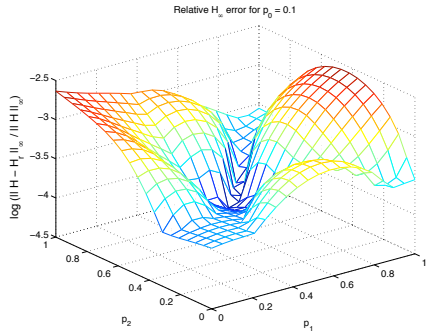

Figure 4: Example 6.1 with $\nu = 3$: relative $\mathcal{H}_\infty$ error as p_1 and p_2 vary.

6.1.1 Comparison with other model reduction approaches

To illustrate the superiority of our piecewise $\mathcal{H}_2$ optimal approach as described in Algorithm 5.1, we compare it with assorted generic interpolatory model reduction methods where the interpolation points do not have the (local) $\mathcal{H}_2$ optimality that Algorithm 5.1 produces. We proceed as follows: For the same parameter sets as above, $\{\mathbf{p}^{(i)}\}_{i=1}^{6}$, we obtain the projection matrices $\mathbf{V}^{(i)}$ and $\mathbf{W}^{(i)}$ using the frequency interpolation points that are used to initiate the optimal $\mathcal{H}_2$ reduction process at each $\mathbf{p}^{(i)}$. In effect, we apply only one-step interpolatory model reduction as opposed to the iterative $\mathcal{H}_2$-optimal (IRKA) process. This is what one would do in a generic interpolation setting by choosing some interpolation points and obtaining the reduced model. We have concatenated $\mathbf{V}^{(i)}$ and $\mathbf{W}^{(i)}$ for $i = 1, \ldots, L$ as Algorithm 5.1 does, and then obtained the corresponding parameterized reduced model. For comparison, we calculate the error at the same grid points used before by fixing p_0 at 0.1 and display the resulting relative $\mathcal{H}_2$ errors and relative $\mathcal{H}_\infty$ error in Figures 7 and 8. The maximum relative $\mathcal{H}_\infty$ errors and relative $\mathcal{H}_2$ errors are, respectively, 4.98×10^{-1} and 2.19×10^{-1}. Note that these relative errors are two orders of magnitude higher than those obtained by the piecewise $\mathcal{H}_2$ optimal approach that we propose. This illustrates clearly the importance of optimal $\mathcal{H}_2$ shift selection in our algorithm. It is useful to note that we have initialized Algorithm 5.1 with the same interpolation points and IRKA (Algorithm 3.1)

Algorithm 4.1. ***PMOR with Interpolatory Projections***

1. *Select "frequencies"* $\sigma_1, \ldots, \sigma_K \in \mathbb{C}$, *parameter vectors* $\mathbf{p}^{(1)}, \ldots, \mathbf{p}^{(L)} \in \mathbb{R}^\nu$, *left tangent directions* $\{\mathbf{c}_{11}, \ldots, \mathbf{c}_{1,L}, \mathbf{c}_{21}, \ldots, \mathbf{c}_{K,L}\} \subset \mathbb{C}^\ell$, *and right tangent directions* $\{\mathbf{b}_{11}, \ldots, \mathbf{b}_{1,L}, \ \mathbf{b}_{21}, \ldots, \mathbf{b}_{K,L}\} \subset \mathbb{C}^m$.

   The order of the reduced model will be $r = K \cdot L$.

2. *Compute a basis* $\{\mathbf{v}_1, \ldots, \mathbf{v}_r\}$ *for*

$$\mathcal{V}_r = \underset{\substack{i=1,\ldots,K \\ j=1,\ldots,L}}{\text{span}} \left\{ \boldsymbol{\mathcal{A}} \left(\sigma_i, \mathbf{p}^{(j)} \right)^{-1} \mathbf{B}(\mathbf{p}^{(j)}) \mathbf{b}_{ij} \right\}.$$

3. *Compute a basis* $\{\mathbf{w}_1, \ldots, \mathbf{w}_r\}$ *for*

$$\mathcal{W}_r = \underset{\substack{i=1,\ldots,K \\ j=1,\ldots,L}}{\text{span}} \left\{ \left(\mathbf{c}_{ij}^T \mathbf{C}(\mathbf{p}^{(j)}) \boldsymbol{\mathcal{A}} \left(\sigma_i, \mathbf{p}^{(j)} \right)^{-1} \right)^T \right\}.$$

4. *Set* $\mathbf{V}_r := [\mathbf{v}_1, \ldots, \mathbf{v}_r]$ *and* $\mathbf{W}_r := [\mathbf{w}_1, \ldots, \mathbf{w}_r]$.

5. *(Pre)compute from (4):* $\mathbf{A}_r(\mathbf{p}) = \mathbf{W}_r^T \mathbf{A}(\mathbf{p}) \mathbf{V}_r$, $\mathbf{E}_r(\mathbf{p}) = \mathbf{W}_r^T \mathbf{E}(\mathbf{p}) \mathbf{V}_r$, $\mathbf{B}_r(\mathbf{p}) = \mathbf{W}_r^T \mathbf{B}(\mathbf{p})$, $\mathbf{C}_r(\mathbf{p}) = \mathbf{C}(\mathbf{p}) \mathbf{V}_r$.

A generic implementation of PMOR using interpolatory projections as described in Theorem 3 is provided in Algorithm 4.1, where we continue to use the notation $\boldsymbol{\mathcal{A}}(s, \mathbf{p}) := s\mathbf{E}(\mathbf{p}) - \mathbf{A}(\mathbf{p})$ as we have above. Note that the number of interpolation frequencies, K, and the number of interpolation points for parameter vectors, L, needs to be chosen *a priori* and the total model order is (nominally) $r = K \cdot L$.

Certainly, the performance of the procedure strongly depends on the choice of interpolation data. A first refinement of this basic approach is to compute frequency points for a fixed selection of parameter vectors that are locally optimal with respect to $\mathcal{H}_2$ error measures using the Iterative Rational Krylov Algorithm (IRKA) as in [25]. Choosing both the frequency and parameter interpolation data as well as the tangent directions in an optimal way will be discussed in the next section.

5 An $\mathcal{H}_2$-based approach to parameterized model reduction

Algorithm 4.1 will produce a parameterized reduced-order model that interpolates the original system in the tangent directions $\mathbf{b}_i$ and $\mathbf{c}_i^T$ at the (complex) frequency σ_i and parameter values, $\hat{\mathbf{p}}_j$. In many problem scenarios, there will be a natural choice of parameter vectors that will be representative of the parameter ranges within which the original system must operate. Sometimes designers will specify important parameter sets in the neighborhood of which reduced-order models should be particularly accurate. In other cases, the physics of the problem will provide some insight to where parameters should be chosen. In all these circumstances, the choice of interpolation data for parameter vectors has been made, leaving open the question of how best to choose the frequency interpolation data. We will give a heuristic approach to resolve this problem using methods for nonparameterized systems that can yield optimal $\mathcal{H}_2$ frequency interpolation points.

Given a full-order parameterized system $\mathbf{H}(s, \mathbf{p})$, suppose L different parameter vectors $\{\mathbf{p}^{(1)}, \ldots, \mathbf{p}^{(L)}\}$ are selected as parameter interpolation points. For each $\mathbf{p}^{(i)}$, define $\mathbf{H}^{(i)}(s) = \mathbf{H}(s, \mathbf{p}^{(i)})$. For each $i = 1, \ldots, L$, $\mathbf{H}^{(i)}$ can be viewed as a (nonparameterized) full-order model and we may apply Algorithm 3.1 to each $\mathbf{H}^{(i)}(s)$ to obtain an $\mathcal{H}_2$ optimal reduced-order model

(say, of order r_i) and corresponding projection subspaces $\mathbf{V}^{(i)} \in \mathbb{R}^{n\times r_i}$ and $\mathbf{W}^{(i)} \in \mathbb{R}^{n\times r_i}$. Let $r = r_1 + r_2 + \cdots r_L$. We concatenate these matrices to get

$$\mathbf{V}_r = [\mathbf{V}^{(1)},\ \mathbf{V}^{(2)},\ \ldots,\ \mathbf{V}^{(L)}] \in \mathbb{R}^{n\times r} \text{ and } \mathbf{W}_r = [\mathbf{W}^{(1)},\ \mathbf{W}^{(2)},\ \ldots,\ \mathbf{W}^{(L)}] \in \mathbb{R}^{n\times r}.$$

This leads to the final parameterized reduced-order model, $\mathbf{H}_r(s,\mathbf{p})$, as in (3). Note that the $\mathbf{H}_r(s,\mathbf{p})$ will not be an $\mathcal{H}_2$ optimal system approximation to $\mathbf{H}(s,\mathbf{p})$ for any parameter choice although it contains L smaller $\mathcal{H}_2$ optimal submodels that can be recovered by truncation of $\mathbf{H}_r$ evaluated at each of the L given parameter vectors. In any case, $\mathbf{H}_r$ still interpolates $\mathbf{H}$ at all parameter choices. A brief sketch of the method is given in Algorithm 5.1. Effectiveness of this algorithm is illustrated with several numerical examples in Section 6.

Algorithm 5.1. Piecewise $\mathcal{H}_2$ Optimal Interpolatory PMOR

1. *Select L parameter vectors $\{\mathbf{p}^{(1)}, \mathbf{p}^{(2)}, \ldots, \mathbf{p}^{(L)}\}$ and reduction orders $\{r_1, r_2, \ldots, r_L\}$.*
2. *For each $i = 1, 2, \ldots, L$ Define the i^{th} system instance: $\mathbf{H}^{(i)}(s) = \mathbf{H}(s, \mathbf{p}^{(i)})$ and apply the optimal $\mathcal{H}_2$ reduction of Algorithm 3.1 to $\mathbf{H}^{(i)}(s)$, constructing interpolating spaces of dimension r_i spanned by $\mathbf{V}^{(i)}$ and $\mathbf{W}^{(i)}$.*
3. *Concatenate $\mathbf{V}^{(i)}$ and $\mathbf{W}^{(i)}$ for $i = 1, \ldots, L$ to obtain the final projection matrices $\mathbf{V}_r$ and $\mathbf{W}_r$ of dimension $r = r_1 + \ldots + r_L$:*

   $$\mathbf{V}_r = [\mathbf{V}^{(1)},\ \mathbf{V}^{(2)},\ \ldots,\ \mathbf{V}^{(L)}] \text{ and } \mathbf{W}_r = [\mathbf{W}^{(1)},\ \mathbf{W}^{(2)},\ \ldots,\ \mathbf{W}^{(L)}].$$

4. *Use an SVD or rank-revealing QR factorization to remove rank-deficient components from $\mathbf{V}_r$ and $\mathbf{W}_r$.*

The final parameterized reduced model is determined by $\mathbf{V}_r$ and $\mathbf{W}_r$ from (3).

The situation becomes harder if we do not have any *a priori* knowledge of particular parameter values that are important but have instead, perhaps only information about allowable parameter ranges within the parameter space. There are methods to address this difficulty. One possible approach is the so-called greedy selection algorithm of Bui-Thanh *et al.* [8]. Even though the final reduced-order model of [8] proves to be a high quality approximation, the optimization algorithm that needs to be solved at each step could be computationally expensive, possibly prohibitively so. Another strategy for an effective and representative choice of parameter points in higher dimensional parameter spaces (for example, say, with $\nu = 10$) comes through the use of sparse grids [9, 23, 49]. This approach is based on a hierarchical basis and a sparse tensor product construction. The dimension of the sparse grid space is of reduced order $\mathcal{O}(2^n n^{\nu-1})$ compared to the dimension of the corresponding full grid space given by $\mathcal{O}(2^{\nu n})$. See [3] for another approach to parameterized model reduction using sparse grids. However, as has been done for optimal $\mathcal{H}_2$ interpolation point selection achieved by the original Algorithm 3.1, a promising goal would be to obtain *optimal parameter selection points* that minimize error measures that are appropriate to parameterized systems. We consider this problem below, for SISO systems with a specific parameter dependency.

5.1 Optimal interpolation for special SISO parameterizations

In the particular case that $\mathbf{H}(s,\mathbf{p})$ is a single input/single output system with the parametric dependence occurring solely in $\mathbf{C}(\mathbf{p})$ and $\mathbf{B}(\mathbf{p})$, we are able to produce reduced-order systems that are optimal with respect to a composite error measure that is an $\mathcal{L}_2$ error relative to parameters

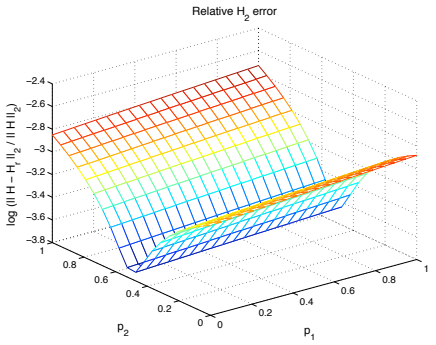

Figure 1: Example 6.1 with $\nu = 2$: relative $\mathcal{H}_2$-error as p_1 and p_2 vary.

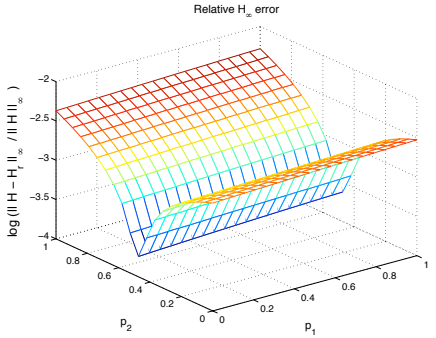

Figure 2: Example 6.1 with $\nu = 2$: relative $\mathcal{H}_\infty$ error as p_1 and p_2 vary.

$p_0 = 0.8$ and add three more choices for p_1 and p_2 for the case $p_0 = 0.1$. Overall, our parameter selection for $\mathbf{p} = [p_0, p_1, p_2]^T$ becomes

$$\begin{array}{lll} \mathbf{p}^{(1)} = [0.8, 0.5, 0.5]^T, & \mathbf{p}^{(2)} = [0.8, 0, 0.5]^T, & \mathbf{p}^{(3)} = [0.8, 1, 0.5]^T, \\ \mathbf{p}^{(4)} = [0.1, 0.5, 0.5]^T, & \mathbf{p}^{(5)} = [0.1, 0, 1]^T, & \mathbf{p}^{(6)} = [0.1, 1, 1]^T. \end{array}$$

As in the two parameter case, we apply Algorithm 5.1 by reducing the order at parameter values $\mathbf{p}^{(i)}$, $i = 1, \ldots, 6$, using $\mathcal{H}_2$ optimal frequency interpolants with orders $r_1 = r_2 = r_3 = 3$ and $r_4 = r_5 = r_6 = 4$. To illustrate the performance of the reduced-order model, we fix p_0 at a specific value, vary the parameters p_1 and p_2 over the full parameter space $[0, 1] \times [0, 1]$, and compute relative $\mathcal{H}_\infty$ error (35) and relative $\mathcal{H}_2$ error (34) at each grid point. We choose the values $p_0 = 0.1$ and $p_0 = 0.5$. Note that $p_0 = 0.5$ is not in the parameter selection set. The error plots for $p_0 = 0.1$ are shown in Figures 3 and 4. As in the two-parameter case, the reduced models approximate the full-order dynamics accurately. The resulting maximum relative $\mathcal{H}_\infty$ error and relative $\mathcal{H}_2$ error for $p_0 = 0.1$ are 2.66×10^{-3} and 2.13×10^{-3}, respectively.

The errors over the full range of p_1 and p_2 are even smaller for $p_0 = 0.5$, as can be seen in Figures 5 and 6. The maximum relative $\mathcal{H}_\infty$ error and relative $\mathcal{H}_2$ error are, respectively, 3.62×10^{-4} and 1.44×10^{-4}, i.e., one order of magnitude smaller than for $p_0 = 0.1$.

6 Numerical Examples

6.1 Convection-diffusion flow in two dimensions

We consider a convection-diffusion equation on the unit square $\Omega = (0,1)^2$:

$$\frac{\partial \mathbf{x}}{\partial t}(t,\xi) = \Delta \mathbf{x}(t,\xi) + \mathbf{p}\cdot\nabla \mathbf{x}(t,\xi) + b(\xi)u(t), \quad \xi \in \Omega,\ t \in (0,\infty),$$

with homogeneous Dirichlet boundary conditions: $\mathbf{x}(t,\xi) = 0, \quad \xi \in \partial\Omega$.

The parameter vector $\mathbf{p} = [p_1, p_2]^T$ determines convective transport in both coordinate directions whereas the function $b(\cdot)$ is the characteristic function of the domain where the input function $u(\cdot)$ acts.

We discretize the convection-diffusion equation with finite differences to obtain a parameterized linear system in state-space form

$$\dot{\mathbf{x}}(t) = (\mathbf{A}_0 + p_1\mathbf{A}_1 + p_2\mathbf{A}_2)\,\mathbf{x}(t) + \mathbf{B}\,u(t), \qquad y(t) = \mathbf{C}\,\mathbf{x}(t), \tag{33}$$

with $\mathbf{A}_0$, $\mathbf{A}_1$, $\mathbf{A}_2 \in \mathbb{R}^{400\times 400}$, $\mathbf{B} \in \mathbb{R}^{400\times 1}$ and $\mathbf{C} \in \mathbb{R}^{1\times 400}$. We assume $\mathbf{B} = \mathbf{e}_1$ (first unit vector) and $\mathbf{C} = \mathbf{e}^T$ (all ones). The parameter range considered is p_1, $p_2 \in [0,\ 1]$.

In this example, the physics of the problem does not provide particular insight to what parameter values might be important. The range of parameter values we consider keep the behaviour of the system diffusion-dominated, so we don't take into account the possible desirability of changing the discretization for different parameter values so as to maintain an upwind bias in the discretization. Motivated by sparse-grid point selection in a two-dimensional space, we use the following level-1 sparse-grid points $\mathbf{p} = [p_1, p_2]^T$ to discretize the parameter space:

$$\mathbf{p}^{(1)} = [0.5, 0.5]^T, \quad \mathbf{p}^{(2)} = [0, 0.5]^T, \quad \mathbf{p}^{(3)} = [1, 0.5]^T, \quad \mathbf{p}^{(4)} = [0.5, 0]^T, \quad \mathbf{p}^{(5)} = [0.5, 1]^T.$$

We further simplify this selection by removing the $\mathbf{p}^{(4)}$ and $\mathbf{p}^{(5)}$ due to symmetry of the problem. Hence, our parameter set becomes $\{\mathbf{p}^{(1)}, \mathbf{p}^{(2)}, \mathbf{p}^{(3)}\}$. We apply Algorithm 5.1 with $r_1 = r_2 = r_3 = 4$ for $\mathbf{p}^{(i)}$, $i = 1, 2, 3$; the final parameterized reduced-order system as defined in (3) has dimension $r = 12$.

A good parameterized reduced-order model needs to represent the full parameterized model with high fidelity for a wide range of parameter values; certainly not just for those values chosen as the interpolation parameters. To illustrate the quality of our parameterized reduced-order models, we evaluate the full-order model, $\mathbf{H}(\cdot, \mathbf{p})$, varying parameter values, $\mathbf{p} = [p_1,\ p_2]^T$, across the full parameter range $[0,1]\times[0,1]$, and compute

$$\text{the relative } \mathcal{H}_2\text{-error at } \mathbf{p} \quad = \quad \frac{\|\mathbf{H}(\cdot,\mathbf{p}) - \mathbf{H}_r(\cdot,\mathbf{p})\|_{\mathcal{H}_2}}{\|\mathbf{H}(\cdot,\mathbf{p})\|_{\mathcal{H}_2}} \ \text{ and} \tag{34}$$

$$\text{the relative } \mathcal{H}_\infty\text{-error at } \mathbf{p} \quad = \quad \frac{\|\mathbf{H}(\cdot,\mathbf{p}) - \mathbf{H}_r(\cdot,\mathbf{p})\|_{\mathcal{H}_\infty}}{\|\mathbf{H}(\cdot,\mathbf{p})\|_{\mathcal{H}_\infty}}. \tag{35}$$

The corresponding mesh plots of relative error are shown in Figures 1 and 2. With a model of order $r = 12$, the maximum relative $\mathcal{H}_\infty$ errors and $\mathcal{H}_2$ errors are, respectively, 5.21×10^{-3} and 1.86×10^{-3}. In terms of either error measure, the reduced-order model is accurate to an order of at least 10^{-3} and we are able to capture the full-order dynamics accurately throughout the whole parameter range.

Next, we add a third parameter p_0 to the model (33) in order to vary the diffusion:

$$\dot{\mathbf{x}}(t) = (p_0\mathbf{A}_0 + p_1\mathbf{A}_1 + p_2\mathbf{A}_2)\,\mathbf{x}(t) + \mathbf{B}\,u(t), \qquad y(t) = \mathbf{C}\,\mathbf{x}(t). \tag{36}$$

The diffusion coefficient p_0 varies in [0.1, 1] and becomes the crucial parameter for smaller values in that range. Hence, we weight our parameter selection as follows. The problem approaches the previous case as p_0 increases to 1. Thus, we keep the same choice for p_1 and p_2 as above for

and $\mathcal{H}_2$ error relative to the system response. To illustrate, we consider a simple two parameter case for a system having the form:

$$\begin{aligned} H(s,\mathbf{p}) =& \mathbf{c}^T(p)\,(s\,\mathbf{E} - \mathbf{A})^{-1}\,\mathbf{b}(q), \\ & \text{with } \mathbf{c}(p) = \mathbf{c}_0 + p\,\mathbf{c}_1 \text{ and } \mathbf{b}(q) = \mathbf{b}_0 + q\,\mathbf{b}_1, \end{aligned} \tag{23}$$

where $\mathbf{p} = [p,\ q]^T$ and $0 \le p,\ q \le 1$. This setting can be generalized in many directions but serves to illustrate the main points.

Denoting $\mathcal{D} = [0,1]\times[0,1]$, define a norm for systems having the form (23):

$$\|H\|^2_{\mathcal{H}_2\otimes\mathcal{L}_2(\mathcal{D})} \stackrel{\text{def}}{=} \frac{1}{2\pi}\int_{-\infty}^{+\infty}\iint_{\mathcal{D}} |H(\imath\omega,\ \mathbf{p})|^2\, dA(\mathbf{p})\, d\omega. \tag{24}$$

Obviously other choices for $\mathcal{D}$ and other measures aside from Lebesgue measure, $dA(\mathbf{p})$ are possible. We seek an *optimal* reduced-order parameterized model, $\widetilde{H}_r(s,\mathbf{p})$, having the same form as $H(s,\mathbf{p})$,

$$\widetilde{H}_r(s,\mathbf{p}) = (\mathbf{c}_{0,r} + p\,\mathbf{c}_{1,r})^T(s\mathbf{E}_r - \mathbf{A}_r)^{-1}(\mathbf{b}_{0,r} + q\,\mathbf{b}_{1,r}), \tag{25}$$

such that

$$\|H - \widetilde{H}_r\|_{\mathcal{H}_2\otimes\mathcal{L}_2(\mathcal{D})} = \min_{\substack{H_r \text{ stable} \\ \text{for all } \mathbf{p}\in\mathcal{D}}} \|H - H_r\|_{\mathcal{H}_2\otimes\mathcal{L}_2(\mathcal{D})}. \tag{26}$$

Theorem 6. *Let $H(s,\mathbf{p})$ be given as in (23) and let $\mathcal{D} = [0,1]\times[0,1]$. Define the auxiliary MIMO transfer function:*

$$\mathfrak{H}(s) = [\mathbf{c}_0,\ \mathbf{c}_1]^T\,(s\,\mathbf{E} - \mathbf{A})^{-1}\,[\mathbf{b}_0,\ \mathbf{b}_1]\,. \tag{27}$$

Then, $\|H\|_{\mathcal{H}_2\otimes\mathcal{L}_2(\mathcal{D})} = \|\mathbf{L}^T\mathfrak{H}\,\mathbf{L}\|_{\mathcal{H}_2}$ where $\mathbf{L} = \begin{bmatrix} 1 & 0 \\ \frac{1}{2} & \frac{1}{2\sqrt{3}} \end{bmatrix}$.

In particular, the norm we have defined on $\mathcal{H}_2\otimes\mathcal{L}_2(\mathcal{D})$ for the parameterized system $H(s,\mathbf{p})$ is equivalent to a (weighted) MIMO $\mathcal{H}_2$ norm for $\mathfrak{H}(s)$.

Proof. Observe that

$$H(s,\mathbf{p}) = [\,1,\ p\,]\,\mathfrak{H}(s)\begin{bmatrix} 1 \\ q \end{bmatrix}. \tag{28}$$

Substitute this expression into (24), rearrange the integrand, and note that $\mathbf{L}$ is the Cholesky factor of $\displaystyle\int_0^1\begin{bmatrix} 1 \\ q \end{bmatrix}[\,1,\ q\,]\,dq = \int_0^1\begin{bmatrix} 1 \\ p \end{bmatrix}[\,1,\ p\,]\,dp = \begin{bmatrix} 1 & \frac{1}{2} \\ \frac{1}{2} & \frac{1}{3} \end{bmatrix} = \mathbf{L}\mathbf{L}^T$. □

Although the model system we consider in (23) has a parameter range restricted to $\mathbf{p} = [p,\ q]^T \in \mathcal{D}$, interpolation is well-defined for parameter values outside of $\mathcal{D}$. Indeed, parameter interpolation will be well-defined even for $p = \infty$ or $q = \infty$: consider for nonzero (but finite) p, q the interpolation condition,

$$\begin{aligned} H(\sigma,\mathbf{p}) =& p\,q\,(\frac{1}{p}\mathbf{c}_0 + \mathbf{c}_1)^T(\sigma\mathbf{E} - \mathbf{A})^{-1}(\frac{1}{q}\mathbf{b}_0 + \mathbf{b}_1) \\ =& p\,q\,(\frac{1}{p}\mathbf{c}_{0,r} + \mathbf{c}_{1,r})^T(\sigma\mathbf{E}_r - \mathbf{A}_r)^{-1}(\frac{1}{q}\mathbf{b}_{0,r} + \mathbf{b}_{1,r}) = H_r(\sigma,\mathbf{p}), \end{aligned}$$

and then let p or q (or both) approach ∞. We interpret the interpolation condition $H(\sigma,[p,\ q]) = H_r(\sigma,[p,\ q])$ for such extended complex values for $\mathbf{p} = [p,\ q]$ as follows:

- $H(\sigma,[\infty,\ q]) = H_r(\sigma,[\infty,\ q])$ with q fixed and finite is interpreted as: $\mathbf{c}_1^T(\sigma\mathbf{E} - \mathbf{A})^{-1}(\mathbf{b}_0 + q\mathbf{b}_1) = \mathbf{c}_{1,r}^T(\sigma\mathbf{E}_r - \mathbf{A}_r)^{-1}(\mathbf{b}_{0,r} + q\mathbf{b}_{1,r})$;
- $H(\sigma,[p,\ \infty]) = H_r(\sigma,[p,\ \infty])$ with p fixed and finite is interpreted as: $(\mathbf{c}_0 + p\mathbf{c}_1)^T(\sigma\mathbf{E} - \mathbf{A})^{-1}\mathbf{b}_1 = (\mathbf{c}_{0,r} + p\mathbf{c}_{1,r})^T(\sigma\mathbf{E}_r - \mathbf{A}_r)^{-1}\mathbf{b}_{1,r}$;

- $H(\sigma,[\infty,\,\infty]) = H_r(\sigma,[\infty,\,\infty])$ is interpreted as:
  $\mathbf{c}_1^T(\sigma\mathbf{E}-\mathbf{A})^{-1}\mathbf{b}_1 = \mathbf{c}_{1,r}^T(\sigma\mathbf{E}_r-\mathbf{A}_r)^{-1}\mathbf{b}_{1,r}$.

Similar extensions can be made for derivative interpolation conditions.

Theorem 6 shows that the least-squares error measure in the $\mathcal{H}_2\otimes\mathcal{L}_2(\mathcal{D})$ norm for the SISO parametric system is indeed a MIMO $\mathcal{H}_2$ norm for a nonparametric linear system. This means we can solve the parametric $\mathcal{H}_2\otimes\mathcal{L}_2(\mathcal{D})$ optimization problem (26) by solving an equivalent nonparametric MIMO $\mathcal{H}_2$ optimization problem which we know how to solve using Theorem 2 and Algorithm 3.1. This leads to the following result:

Theorem 7. *Let $H(s,\mathbf{p})$ be given as in (23). Suppose a parameterized reduced-order model $\widetilde{H}_r(s,\mathbf{p})$ of the form (25) minimizes $\|H-H_r\|_{\mathcal{H}_2\otimes\mathcal{L}_2(\mathcal{D})}$ over all (stable) rth-order transfer functions and that the associated reduced-order pencil $s\mathbf{E}_r-\mathbf{A}_r$ has only simple eigenvalues $\{\widetilde{\lambda}_i\}_{i=1}^r$. Then there are optimal frequency shifts, $\{-\widetilde{\lambda}_i\}_{i=1}^r$, and optimal parameter interpolation vectors, $\{\widetilde{\mathbf{p}}_i\}_{i=1}^r$ such that*

$$H(-\widetilde{\lambda}_i,\,\widetilde{\mathbf{p}}_i) = \widetilde{H}_r(-\widetilde{\lambda}_i,\,\widetilde{\mathbf{p}}_i), \qquad \frac{\partial}{\partial s}H(-\widetilde{\lambda}_i,\,\widetilde{\mathbf{p}}_i) = \frac{\partial}{\partial s}\widetilde{H}_r(-\widetilde{\lambda}_i,\,\widetilde{\mathbf{p}}_i),$$
$$\text{and}\quad \nabla_{\mathbf{p}}H(-\widetilde{\lambda}_i,\,\widetilde{\mathbf{p}}_i) = \nabla_{\mathbf{p}}\widetilde{H}_r(-\widetilde{\lambda}_i,\,\widetilde{\mathbf{p}}_i), \tag{29}$$

for $i=1,\,\ldots,\,r$.

Proof. Define a reduced-order MIMO system associated with $\widetilde{H}_r$:

$$\widetilde{\mathcal{H}}_r(s) = [\mathbf{c}_{0,r},\,\mathbf{c}_{1,r}]^T\,(s\,\mathbf{E}_r\,-\,\mathbf{A}_r)^{-1}\,[\mathbf{b}_{0,r},\,\mathbf{b}_{1,r}]\,.$$

Analogously to (28), we have

$$\widetilde{H}_r(s,\mathbf{p}) = [\,1,\;p\,]\,\widetilde{\mathcal{H}}_r(s)\begin{bmatrix}1\\ q\end{bmatrix}.$$

Since $\widetilde{H}_r(s,\mathbf{p})$ minimizes the $\mathcal{H}_2\otimes\mathcal{L}_2(\mathcal{D})$ error from the original system $H(s,\mathbf{p})$, we find an equivalent weighted $\mathcal{H}_2$ approximation problem:

$$\|\mathbf{L}^T\mathcal{H}\,\mathbf{L}-\mathbf{L}^T\widetilde{\mathcal{H}}_r\mathbf{L}\|_{\mathcal{H}_2} = \|H-\widetilde{H}_r\|_{\mathcal{H}_2\otimes\mathcal{L}_2} = \min_{H_r\text{ is stable}}\|H-H_r\|_{\mathcal{H}_2\otimes\mathcal{L}_2}$$
$$= \min_{\mathcal{H}_r\text{ is stable}}\|\mathbf{L}^T\mathcal{H}\,\mathbf{L}-\mathbf{L}^T\mathcal{H}_r\mathbf{L}\|_{\mathcal{H}_2}.$$

Thus, $\mathbf{L}^T\widetilde{\mathcal{H}}_r(s)\mathbf{L}$ is an $\mathcal{H}_2$ optimal reduced-order approximation to the associated MIMO system $\mathbf{L}^T\mathcal{H}(s)\mathbf{L}$. Since the reduced-order pencil $s\mathbf{E}_r-\mathbf{A}_r$ has only simple eigenvalues, $\mathbf{L}^T\widetilde{\mathcal{H}}_r(s)\mathbf{L}$ has a partial fraction expansion,

$$\mathbf{L}^T\widetilde{\mathcal{H}}_r(s)\mathbf{L} = \sum_{i=1}^{r}\frac{1}{s-\widetilde{\lambda}_i}\widetilde{\mathbf{c}}_i\widetilde{\mathbf{b}}_i^T,$$

with $\widetilde{\mathbf{c}}_i,\,\widetilde{\mathbf{b}}_i\in\mathbb{C}^2$ for $i=1,\ldots,r$. This reduced-order MIMO system must satisfy tangential interpolation conditions that are necessary consequences of $\mathcal{H}_2$ optimality:

$$\mathbf{L}^T\mathcal{H}(-\widetilde{\lambda}_i)\mathbf{L}\widetilde{\mathbf{b}}_i = \mathbf{L}^T\widetilde{\mathcal{H}}_r(-\widetilde{\lambda}_i)\mathbf{L}\widetilde{\mathbf{b}}_i,$$
$$\widetilde{\mathbf{c}}_i^T\mathbf{L}^T\mathcal{H}(-\widetilde{\lambda}_i)\mathbf{L} = \widetilde{\mathbf{c}}_i^T\mathbf{L}^T\widetilde{\mathcal{H}}_r(-\widetilde{\lambda}_i)\mathbf{L},$$
$$\text{and}\quad \frac{\partial}{\partial s}\widetilde{\mathbf{c}}_i^T\mathbf{L}^T\mathcal{H}(-\widetilde{\lambda}_i)\mathbf{L}\widetilde{\mathbf{b}}_i = \frac{\partial}{\partial s}\widetilde{\mathbf{c}}_i^T\mathbf{L}^T\widetilde{\mathcal{H}}_r(-\widetilde{\lambda}_i)\mathbf{L}\widetilde{\mathbf{b}}_i. \tag{30}$$

Define for $i=1,\,\ldots,\,r$,

$$\widetilde{\mathbf{c}}_i^T\mathbf{L}^T = [\mu_i,\,\alpha_i] \quad\text{and}\quad \mathbf{L}\widetilde{\mathbf{b}}_i = \begin{bmatrix}\nu_i\\ \beta_i\end{bmatrix}, \tag{31}$$

and associated optimal parameter values:

$$p_i = \alpha_i/\mu_i, \quad\text{and}\quad q_i = \beta_i/\nu_i. \tag{32}$$

For $\mu_i\neq 0$ and $\nu_i\neq 0$, we may simplify (30) as

$$\nu_i\mathcal{H}(-\widetilde{\lambda}_i)\begin{bmatrix}1\\ q_i\end{bmatrix} = \nu_i\widetilde{\mathcal{H}}_r(-\widetilde{\lambda}_i)\begin{bmatrix}1\\ q_i\end{bmatrix},$$
$$\mu_i\,[1,\,p_i]\,\mathcal{H}(-\widetilde{\lambda}_i) = \mu_i\,[1,\,p_i]\,\widetilde{\mathcal{H}}_r(-\widetilde{\lambda}_i),\quad\text{and}$$
$$\mu_i\nu_i\,[1,\,p_i]\left[\frac{\partial\mathcal{H}}{\partial s}(-\widetilde{\lambda}_i)\right]\begin{bmatrix}1\\ q_i\end{bmatrix} = \mu_i\nu_i\,[1,\,p_i]\left[\frac{\partial\widetilde{\mathcal{H}}_r}{\partial s}(-\widetilde{\lambda}_i)\right]\begin{bmatrix}1\\ q_i\end{bmatrix},$$

which leads immediately to the conditions (29). If either $\mu_i=0$ or $\nu_i=0$ (or both), then either p_i or q_i (or both) could take the value ∞ and the interpolation conditions (30) are equivalent to interpolation conditions given above for extended complex values of parameter values. □

Note that the optimal parameter interpolation points $\widetilde{\mathbf{p}}_i=[p_i,\,q_i]^T$ in Theorem 7 are *not* necessarily contained in $\mathcal{D}$, although if $\widetilde{H}_r(s,[0,\,0])$ is a minimal realization, then at least all of them can be guaranteed to be finite.

The definitions in (31) and (32) will be used in Algorithm 5.2 for the computation of an optimal parameterized reduced-order SISO system having the special form (25). Using the results of Theorem 7, Algorithm 5.2 first converts the SISO parameterized model reduction problem in $\mathcal{H}_2\otimes\mathcal{L}_2(\mathcal{D})$ to an equivalent (nonparametrized) MIMO $\mathcal{H}_2$ model reduction problem. Algorithm 3.1 provides frequency interpolation points and tangent directions. Optimal parameter interpolation points are then recovered using (31) and (32), yielding in the end an optimal parameterized reduced model for the original problem with respect to the $\mathcal{H}_2\otimes\mathcal{L}_2(\mathcal{D})$ norm.

Algorithm 5.2. Optimal Interpolation for SISO parameterizations with $H(s,\mathbf{p}) = (\mathbf{c}_0+p\,\mathbf{c}_1)^T\,(s\,\mathbf{E}\,-\,\mathbf{A})^{-1}\,(\mathbf{b}_0+q\,\mathbf{b}_1)$

1. *Construct $\widetilde{\mathbf{H}}(s)$ as in (27) and $\mathbf{L}$ as in Theorem 6.*
2. *Apply Algorithm 3.1 to find an $\mathcal{H}_2$ optimal r^{th}-order approximant to $\mathbf{L}^T\widetilde{\mathbf{H}}(s)\mathbf{L}$. Let $\widetilde{\mathbf{c}}_i$ and $\widetilde{\mathbf{b}}_i$, for $i=1,\ldots,r$ denote the resulting optimal left and right tangent directions, respectively. Also, let $\widetilde{\lambda}_i$ denote the resulting reduced-order poles.*
3. *Compute p_i and q_i for $i=1,\ldots,r$ using (31), (32).*
4. *Construct $\mathbf{V}_r$ and $\mathbf{W}_r$ as in lines 2.-4. in Algorithm 4.1 using $\widetilde{\mathbf{p}}_i=[p_i,\,q_i]^T$ as optimal parameter interpolation points, $\sigma_i=-\widetilde{\lambda}_i$ as frequency interpolation points, $\widetilde{\mathbf{c}}_i$ and $\widetilde{\mathbf{b}}_i$ as left and right tangent directions for $i=1,\ldots,r$.*

The final optimal parameterized reduced-order model is determined from (3).